Highly Functionalized Ferrocenes

Emmanuel Lerayer, Léa Radal, Tuan Anh Nguyen, Nejib Dwadnia, Hélène Cattey, Régine Amardeil, Nadine Pirio, Julien Roger, Jean-Cyrille Hierso

Highly Functionalized Ferrocenes

Emmanuel Lerayer,[a] Léa Radal,[a] Tuan Anh Nguyen,[a] Nejib Dwadnia,[a] Hélène Cattey,[a] Régine Amardeil,[a] Nadine Pirio,[a] Julien Roger,[a] and Jean-Cyrille Hierso*[a,b]

This paper is dedicated to Prof. Roger Guilard for his contribution to the excellence of Coordination Chemistry in France

Abstract: Ferrocene is unique among organometallic compounds, and serves notably as a versatile platform towards the production of ligands useful to promote transition metals chemistry. A general limiting aspect of the synthesis of ferrocene derivatives is the efficient access to sophisticated highly functionalized polysubstituted ferrocenes, *i. e.* bearing four or more substituents replacing hydrogen atoms on the cyclopentadienyl rings. These ferrocene derivatives can bear various functional or/and structuring spectator substituents. Their preparation involves synthetic difficulties resulting from the need of multiple functionalizations coexisting altogether, and satisfying functional group compatibility and high selectivity issues. In the last decades, our group initially designed highly functionalized polyphosphines and hybrid ligands (1,1',3,3'-tetrafunctionalized Fc) using dialkylated 1,1'-*tert*-butylferrocene as a scaffold, which opened the way to various new classes of hybrid compounds. Some of these original ferrocenes were used as ligands, promoting metal catalysed C–C and C–X bond formation (X = O, S, N, *etc.*). Thus, highly functionalized ferrocenes, which include notably (P,P,P,P)-, (P,P,N,N)-, (P,P,P')-, (P,P,B)-, (P,B)- and (N,B)-compounds were developed in which the heteroatoms coexist in a close proximity on a common ferrocene platform with a controlled conformation. The present review details the concepts attached to the synthesis of these highly functionalized ferrocene species, and illustrates their main features and applications related to organometallic chemistry directed towards organic synthesis by metal catalysis.

1. Introduction, "Personal" Historical Perspective and Scope

Air stable, thermodynamically robust, electroactive, soluble in many organic solvents, easily modifiable by convenient synthetic methods, the ferrocene (Fc) backbone is unique among organometallic compounds, including among the metallocenes family.[1–3] The outstanding structuring potential of ferrocene, as a multi-functionalizable platform, allows assembling donor (and acceptor) heteroatoms *via* C–H bond replacement by a great variety of C–X bonds (where *X = B, N, O, P, Si, Se, As, F, Cl, Br, I* and many others). The functionalization of cyclopentadienyl (Cp) rings in ferrocene derivatives has been initially focused on the efficient and practical synthesis of mono- and difunctionalized compounds. From these species, ferrocenyl mono- and diphosphines – including the ubiquitous 1,1'-bis(diphenylphosphino)ferrocene (dppf) – provided the impetus for the development of ferrocene-based ligand chemistry since the 1950's. Owing to their usefulness in homogeneous catalysis for fine chemistry, ferrocene derivatives were used for assisting metal-catalyzed C–C bond and C–X bond formation, including in challenging asymmetric approaches.[4–6] Because the ferrocene backbone can valuably transfer its geometric and electronic features (including chirality and redox behavior) to the polyfunctionalized compounds which are synthesized from it, the development of its functionalization chemistry is very attractive.

In France, following the works on ferrocenes which were conducted by pioneers from the Universities of Dijon and Rennes including –non-exhaustively–[7] J. Tirouflet, R. Dabard, P. H. Dixneuf, D. Astruc,[8–11] the group of B. Gautheron initiated before 2000[12] the polyphosphine studies developed by our group.

In the present account we focused on the synthesis and applications of highly functionalized ferrocenyl derivatives, mainly phosphine derivatives that we developed in our group for the last fifteen years (2003-2018). These polyfunctionalized synthetic targets are challenging, and as such their syntheses were rather scarcely addressed by the others groups which are mentioned in the reviews and book chapters above quoted.[1–6,8–12] Two specificities of our work is that it generally deals not with optically active ferrocenes, and that the emphasis is put on the development of rather sophisticated species bearing at least four (or more) functionalizations out of the ten positions available on the two Cp rings of ferrocene. Along the years, an important objective has been the systematic study of the control of the ferrocene conformation by using additional bulky groups (alkyl groups such as *tert*-butyl or surrogates) and the physicochemical and reactivity consequences. These issues are discussed herein.

2. Ferrocenyl phosphines

Examination of the literature before 2004 reveals that only a few ferrocenyl polyphosphine ligands of higher rank than diphosphines are available for use as ligands in synthetic chemistry and homogeneous catalysis.[13,14] Some seminal works of our group are detailed in a tutorial review on ferrocenyl polyphosphine multidentate effects.[15]

[a] Dr. E. Lerayer, L. Radal, T. A. Nguyen, Dr. N. Dwadnia, Dr. H. Cattey, Dr. R. Amardeil, Prof. Dr. N. Pirio, Dr. J. Roger, Prof. Dr. J.-C. Hierso
Institut de Chimie Moléculaire de l'Université de Bourgogne (ICMUB) UMR CNRS 6302
Université de Bourgogne Franche-Comté (UBFC)
9 avenue Alain Savary, 21078 Dijon, France
E-mail:hiersojc@u-bourgogne.fr
Homepage: http://www.icmub.com/en/members-en/hierso-jean-cyrille.html
[b] Prof. Dr. J.-C. Hierso
Institut Universitaire de France (IUF)

2.1. Tetraphosphines

2.1.1. Synthesis by a direct functionalization of the ferrocene backbone

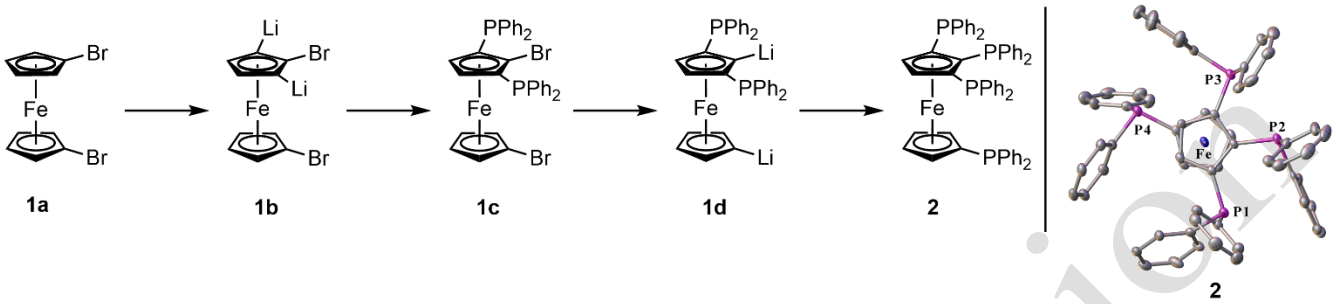

Figure 1. Synthesis of 1,1',2,3-tetraphosphine **2**.

The synthesis of ferrocenyl polyphosphines by direct functionalization of ferrocene backbone has been described by the Butler group,[16] for which a typical illustration is the synthesis of the polydentate ligand 1,1',2,3-tetrakis(diphenylphosphino)ferrocene **2** (Figure 1).[17] This tetraphosphine is obtained starting from the addition of 1,1'-dibromoferrocene **1a** to freshly prepared LDA. Compound **1b** is formed and quenched with chlorodiphenylphosphine to get [1,1′-dibromo-2,5-bis(diphenylphosphino)]ferrocene **1c** in 55% (Figure 1). 1,1′,2,3-tetrakis(diphenylphosphino)ferrocene **2** is obtained in 90% yield from **1d** reacted with $ClPPh_2$. We studied jointly with Butler group the coordination chemistry of **2** towards palladium and nickel. From $PdCl_2L$ (L = COD, $(RCN)_2$) dinuclear species easily formed, while from nickel halides only mononuclear species were identified. The rotational flexibility of this tetraphosphine ligand was evidenced by comparing the XRD structures of **2** and dinuclear palladium complex **2–$(PdCl_2)_2$** (Figs. 1 and 2). The coordination chemistry of **2** clearly combines individual classical schemes of 1,2- and 1,1'-chelating ferrocenyl diphosphines. However, based on ferrocenyl tetraphosphines our group envisioned the development of a more cooperative polydentate ligand chemistry on the metal center, achieved by tri- or tetra-coordination at the same metal center.

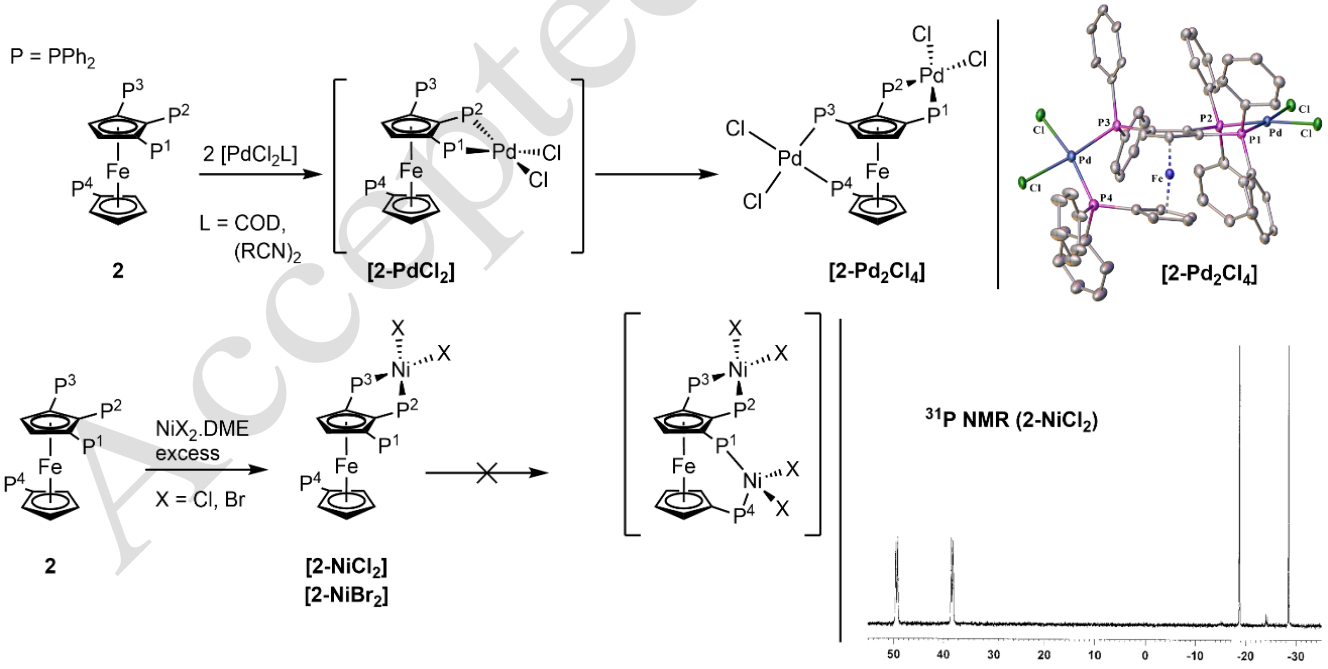

Figure 2. Complexation of 1,1',2,3-tetraphosphine **2** with palladium and nickel halide salts.

An important prerequisite for the coordination of three or more donors at the same metal center,[15] is the adequate geometrical/sterical control of the ferrocene ligand conformation. We thus explored the coordination chemistry of hindered alkylated tetraphosphines originally designed by Broussier and Gautheron (Figure 3).[18–20]

2.1.2. Synthesis by the assembly of adequately substituted cyclopentadienyl rings

The assembly with $Fe^{II}Cl_2$ of cyclopentadienyl lithium **A**, which is obtained *via* a multistep synthesis involving two sequential lithiation/phosphination reactions of 1,2,3-trimethylcyclopenta-1,3-diene, provides the methylated 1,1',2,2'-tetraphosphine **3** in 83% (Fig. 3).[19] The *tert*-butylated cyclopentadienyl **B** is obtained from sequential lithiation/phosphination reactions of dimethylfulvene and was also employed with $Fe^{II}Cl_2$ to form the 1,1',2,2'-tetraphosphine **4** in 70% (Figure 3).[20] The diphosphino functionalization of Cp ring in **B** is highly selective, and directed by both the electronic and steric effects of *tert*-butyl group.

For the phosphines **3** and **4**, both solution ^{31}P NMR and single crystal XRD analyses showed that the structure and conformation adopted by these compounds are very different. Tetraphosphine **3** can be viewed as a bis(diphosphine) for which all the phosphorous atoms in solution NMR are chemically and magnetically equivalent. Consistently, XRD structure analysis indicates a symmetrical structure distributing the phosphino groups as far as possible from each other. Conversely, the solution ^{31}P NMR of **4** revealed a rare AA'BB' phosphorus spin system in which two pairs of P-nuclei (central 1,1'-P and peripheral 2,2'-P) are magnetically inequivalent with strong mutual spin-spin couplings. A large nuclear spin-spin coupling (J_{PP} = 59 Hz, Fig. 3) related to the eclipsed mutual position of central phosphorus is conveyed by their lone pair sharing the same space in a proximity forced by the global conformation constraint.[21,22] Such non covalently bonding $^{31}P\cdots^{31}P$ nuclear spin $^{TS}J_{PP}$ interactions occur through-space,[23] and since our work, have been widely recognized as a fairly common phenomenon in highly constrained dissymmetric diphosphines.[24–27] This constrained proximity is also necessary to induce phosphorus cooperative behavior. This favors the stabilization of robust complexes, and consequently promotes low loading metal catalysis for high turnover numbers (TONs). Accordingly, tetraphosphine **4** promotes palladium catalyzed Suzuki cross-coupling and Heck vinylation reaction with TONs up to 1 000 000.[28]

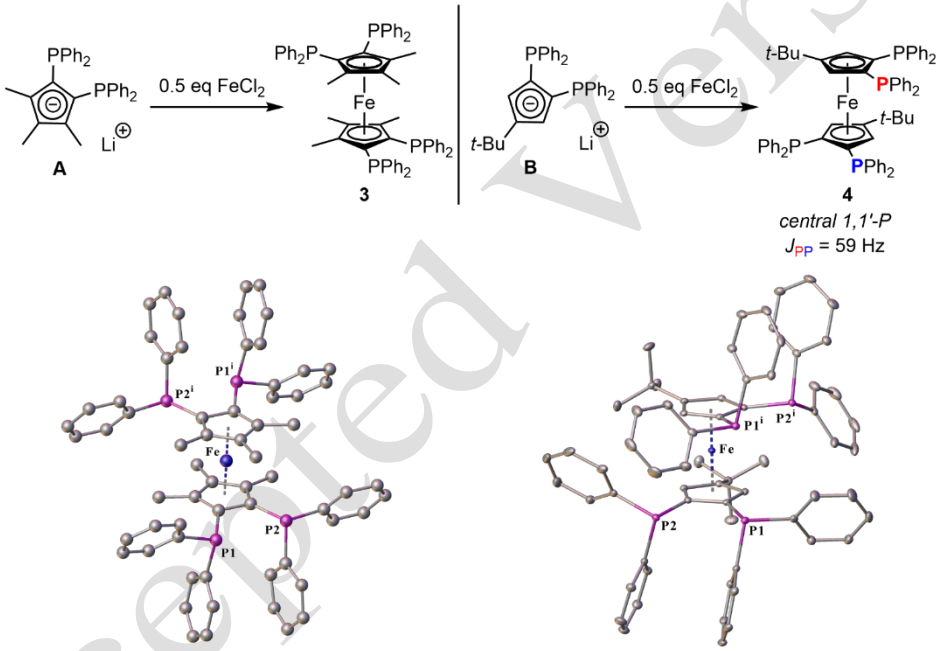

Figure 3. Synthesis of symmetrical tetraphosphines **3** [symmetry transformation: (i) 1-x, 1-y, 1-z] and **4** [symmetry transformation: (i) -x, y, 3/2-z].

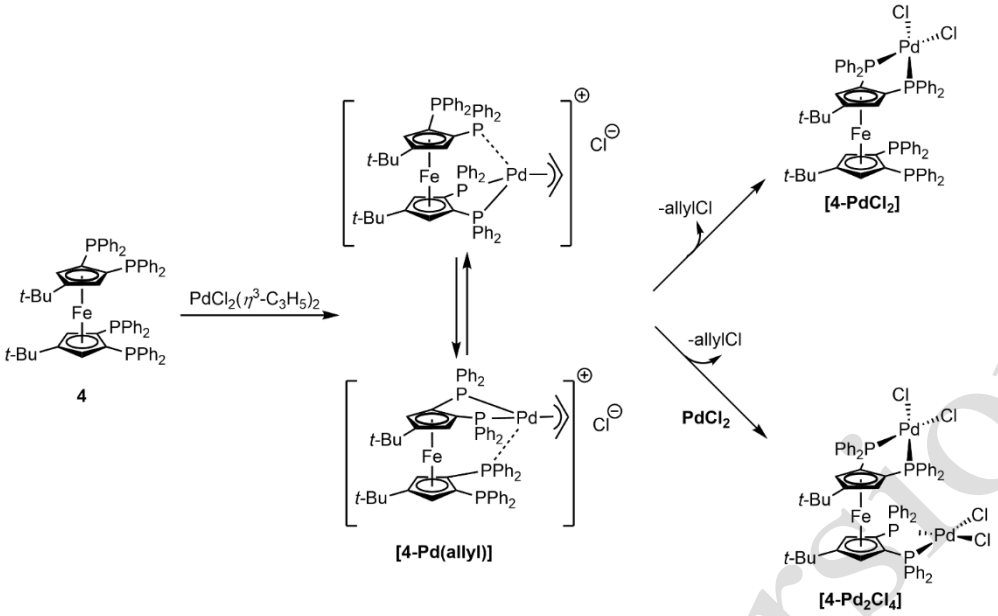

Figure 4. Dynamic three-coordinate complexation of tetraphosphine **4** with palladium.

The coordination chemistry of tetraphosphines **3** with group 6 (Cr, Mo, W) and 7 (Mn) metals,[29] and of **4** with copper[30] and gold[31] was thoroughly studied. However, the interactions between tetraphosphine **4** and group 10 metals (Ni, Pd, Pt)[21] remains the most striking. A dynamic evolution from initially formed labile [**4–Pd(allyl)**] species (Figure 4) towards the well-defined, stable, and non-fluxional complexes [**4–PdCl$_2$**] and [**4–(PdCl$_2$)$_2$**] was observed.[28] The dynamics of such unique interactions in polydentate ligands between the palladium metal center and the four phosphorus atoms has been studied,[32] and exploited in C–C cross coupling at low-palladium catalyst loading. The catalytic system combining the ferrocenyl tetraphosphine **4** and [PdCl(allyl)]$_2$ promotes the cross-coupling of aryl halides with aryl boronic acids (Suzuki reaction) and the vinylation of aryl halides with alkenes (Heck reaction) in the presence of 1.0 to 0.01% metal, while more reactive aryl bromides were reacted with aryl boronic acids or alkenes in the presence of 0.01 to 0.0001% catalyst (corresponding to catalysts TONs up to 10^4-10^6).[28]

In relation with these cross-coupling reactions, kinetic studies based on electrochemical measurements were operated from the catalytically competent mononuclear complexes [**4–PdCl$_2$**] and its analogue [**4–PdBr$_2$**]. We originally measured the rate of Ph–I oxidative addition (O. A.) on electrochemically generated [**4–Pd^0**].[33] In comparison with the systems combining [Pd^0/nPPh$_3$] (n = 2–4) reported by Jutand and Amatore groups (Fig. 5, eq. 1), we find a half-reaction time of $t_{1/2}$ = 130±10 ms (Figure 5, eq. 2).[34,35] The measurements established thus that [**4–Pd^0**] combines an excellent reactivity towards oxidative addition –since the classical pre-catalyst [Pd^0(PPh$_3$)$_4$] has $t_{1/2}$= 30 s, 200 fold slower– with a strongly enhanced stability compared to the low-coordinated reactive species "Pd^0(PPh$_3$)$_2$" for which $t_{1/2}$ = 80 ms (i.e. 1.5 times faster and thus highly unstable Pd^0). We further investigated the addition of aryl bromide and alkyl chloride substrates that are the true substrates used in couplings achieved by [**4–Pd^0**] catalyst.[36] Kinetic constants for the oxidative addition of haloarenes to Pd^0 intermediates generated by electrochemical reduction of [**4–PdCl$_2$**] and [**4–PdBr$_2$**] was found to be: k_{app}(Ph−Br) = 0.48 (in mol^{-1} L s^{-1}) > k_{app}(ClCH$_2$−Cl) = 0.25 ≫ k_{app}(*p*-MeC$_6$H$_4$−Br) = 0.08 ≈ k_{app}(*o*-MeC$_6$H$_4$−Br) = 0.07 ≫ k_{app} (Ph−Cl) (Fig. 5, eq. 3–7).[36]

Kinetic measurements clarified the fact that the presence of supplementary phosphorus atoms (three and four) in polyphosphines of the type of **4** stabilizes Pd^0 molecular complexes, and consequently slows down the O.A. of aryl halides to Pd^0 by at least two orders of magnitude compared to diphosphine coordination. Conversely, these polydentate ligands efficiently inhibit the decoordination of palladium and deleterious formation of palladium black colloids. This work also evidenced the perfect stereoselectivity of the oxidative addition reactions which is induced by the tetraphosphine ligand **4**.[37]

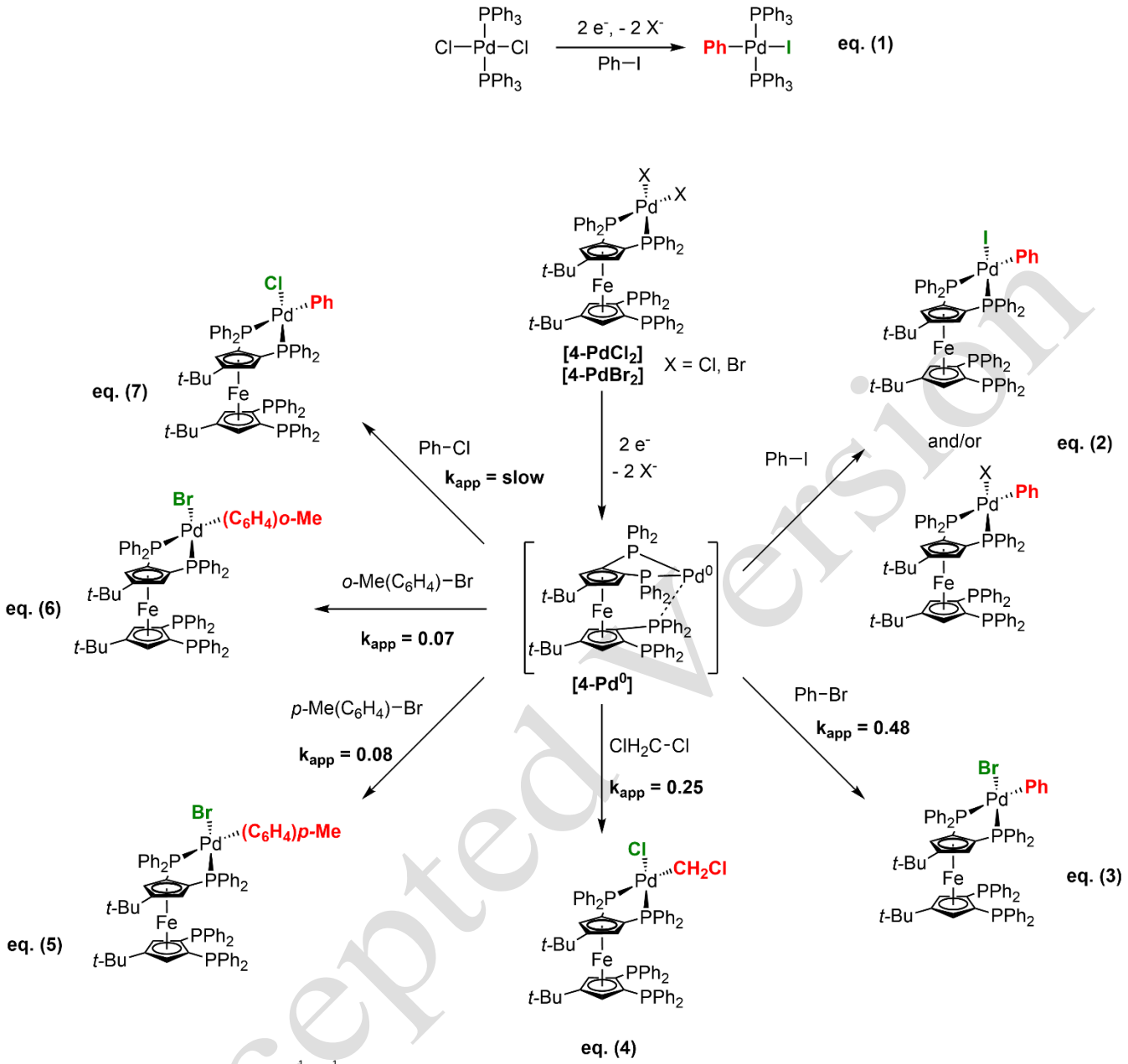

Figure 5. Kinetic Constants k_{app} (in $mol^{-1}.L.s^{-1}$) for O.A. of phenyl bromide and methyl-substituted derivatives to a tetraphosphine-stabilized Pd(0) complex

The proximity of phosphorus atoms in **4** was also originally exploited in zirconium coordination chemistry.[38] A unique mixed ferrocenyl diphosphonium-diphosphine dication **5**, associated with two $[ZrCl_5{\cdot}thf]^-$ anions was obtained as a rare didentate ionic metalloligand. A perfectly selective bis-protonation reaction induced by $ZrCl_4$ in THF was observed (Figure 6). This reactivity was not obtained from organic acids like triflic acid, from which the expected tetraphosphonium salt is obtained. The use of a non-metallocene zirconium chloride adduct in THF as a selective protonation (or "auto-protonation") agent for a polyphosphine ligand involve both carbon–oxygen bond cleavage and carbon–hydrogen activation of THF at ambient temperature in a short period of time (Figure 6, bottom).

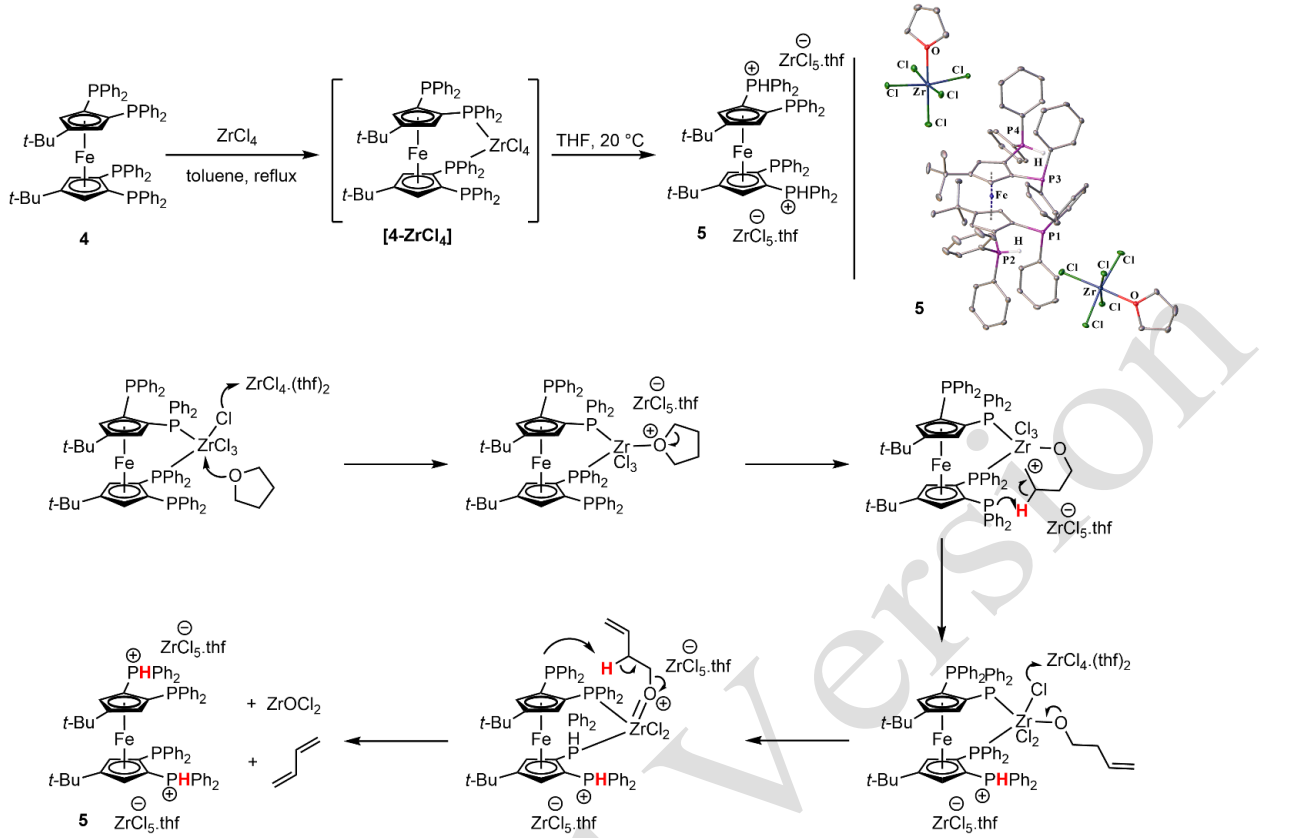

Figure 6. Synthesis and molecular structure of **5**. Proposal for concerted selective formation of complex **5** from tetraphosphine **4**.

The assembly of adequately substituted cyclopentadienyl rings (**C**-**E**, Figure 7) allowed a large extension of the family of tetraphosphine ligand **4** with the conservation of the specific cisoid conformation, in which, for instance, acetal functionalized tetraphosphines **6** and its aldehyde derivative **7** displayed in ^{31}P NMR an AA'BB' spin system. This conformation of ferrocenyl phosphines was controlled by the introduction of *gem*-methyl groups which play the role attributed to *tert*-butyl substituents in **4** and ensure the mutual proximity of the phosphorus atoms in **6** and **7**. Accordingly, the existence of a strong through-space spin-spin coupling ($^{TS}J_{PP}$ = 64.3 Hz and 61.0 Hz, respectively) between internal heteroannular AA' pairs of P-atoms is due to the overlapping of their lone pairs. Such spin couplings attest for the ligand conformation in solution.[39] Tetraphosphine **7** was modified to give the functionalized polyphosphines **8**-**11** (Figure 8). The carbonyl derivative **7** can be grafted directly on preformed Merrifield-type resins. Styrenyl moieties (**9**, **10**) allow for processing tetraphosphine immobilization by co-polymerization with styrene, and alkyltriethoxysilane (**11** obtained from **8**) allow sol-gel mediated anchoring of the ligands on inorganic supports like silica.

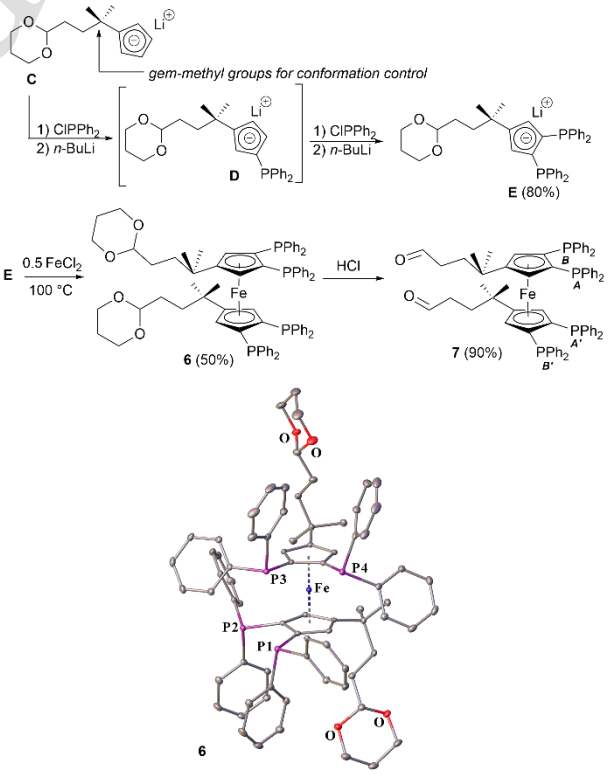

Figure 7. Synthesis and molecular structure of protected tetraphosphine **6** and dialdehyde **7**.

The monofunctionalized analogues **12**-**14** and the vinyl difunctionalized tetraphosphines **15** (Fig. 8) were also

synthesized following the method of assembling adequately substituted Cp rings.[39] One aim was to increase the flexibility of the anchoring upon immobilization (**12**-**14**, being not cross-linking species) or to generate a short cross-linker tetraphosphine (**15**). These functionalized ligands have been incorporated into polystyrene to give either soluble or insoluble polymers, and on inorganic supports such as silica. We reported the catalytic performance in C–C bond formation (Suzuki and Sonogashira reactions, and difficult C–H functionalization of heteroaromatics with demanding chloroarenes) at 0.05–0.5 mol% low palladium loading of the immobilized polyphosphine ligands.[40] They showed excellent performance and good potential for recycling up to six successive runs limited because of accumulative loss of material during filtration. When used with chloroarenes the resulting cumulative turnover numbers of the heterogeneous catalytic systems were found to be satisfactory relative to their homogeneous counterparts tetraphosphine (TONs = 270–1700). Nevertheless, the TONs over 10^4 obtained in coupling bromoarenes under homogeneous conditions was not reached by the supported ligands.[40]

Another conceptual interest of the back-modified tetraphosphine ligands was illustrated with the first ^{31}P NMR ABCD spin systems reported for tetraphosphine **12** (Fig. 8). The simulation of its second order spectrum (Figure 9) evidenced four different but proximate chemical shifts (δ_A = –33.9, δ_B = –29.9, δ_C = –30.3, δ_D = –34.0, with J_{AB} = 73.3 Hz, J_{BC} = 61.6 Hz and J_{CD} = 74.2 Hz, all other coupling constants involved in the ABCD spin system being null. These $^3J_{AB}$, $^3J_{CD}$ and $^{TS}J_{BC}$, are fully consistent with the values obtained for $^{TS}J_{AA}$ and $^3J_{AB}$ = $^3J_{A'B'}$ in the symmetrical ferrocenyl phosphine analogues **3** and **4**.

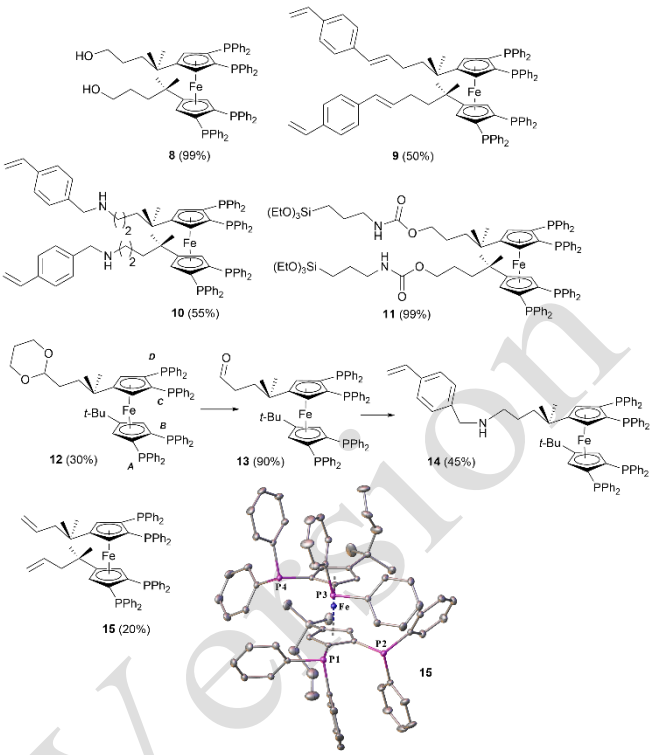

Figure 8. Tail-functionalized tetraphosphines **8**-**15** "ready for immobilization" on various supports.

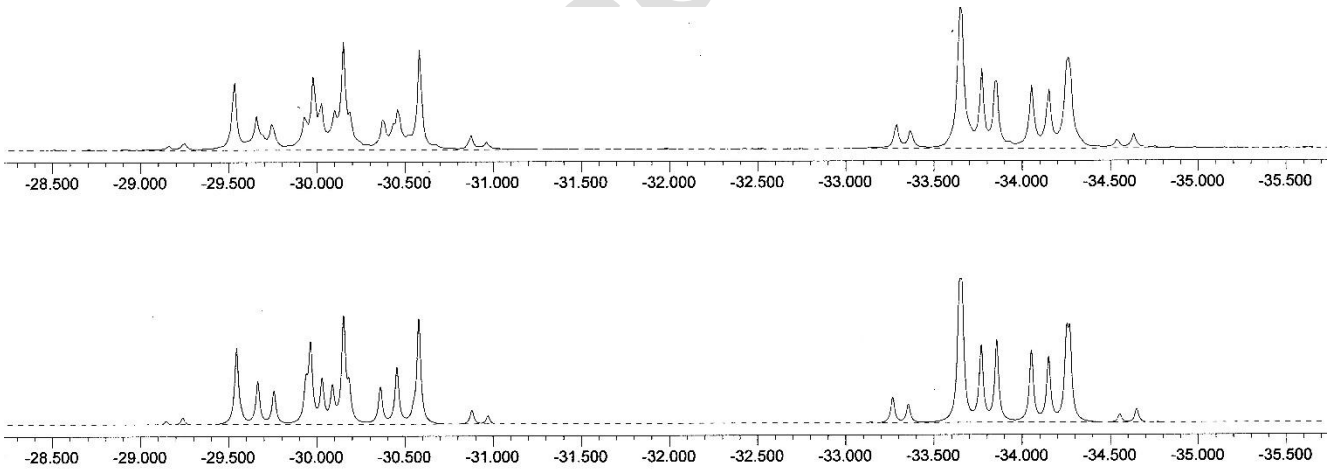

Figure 9. Unique **ABCD** ^{31}P NMR spin system for tetraphosphine **12**: experimental (top) and simulated spectra (bottom).

The controlled conformation and cooperative behavior in complexes formed from *tert*-butylated-tetraphosphines allowed relevant advances in both conceptual understanding of ^{31}P nuclear spin-spin coupling chemical physics,[25] and palladium or palladium/copper catalysis.[30,41] The coordination chemistry of bis(diphosphine) such as ligand **16** (Figure 10),[42] obtained in 73% from **F**, was also found to be useful. Indeed, binuclear palladium complexes derived from **16** where palladium centers are coordinated in a bis-κ^2 mode (XRD in Fig 10) have been identified as competent intermediates in C–S bond formation. The complex [**16–Pd$_2$(CHCl)$_2$Cl$_2$**] displays a binuclear coordination, resembling the 1,1'-P-coordination of dppf and its derivatives. This coordination mode, which involves heteroannular (bridging) coordination with a large bite angle, is related to the high reactivity of such complexes found in the reductive elimination of heteroaromatic thioethers.

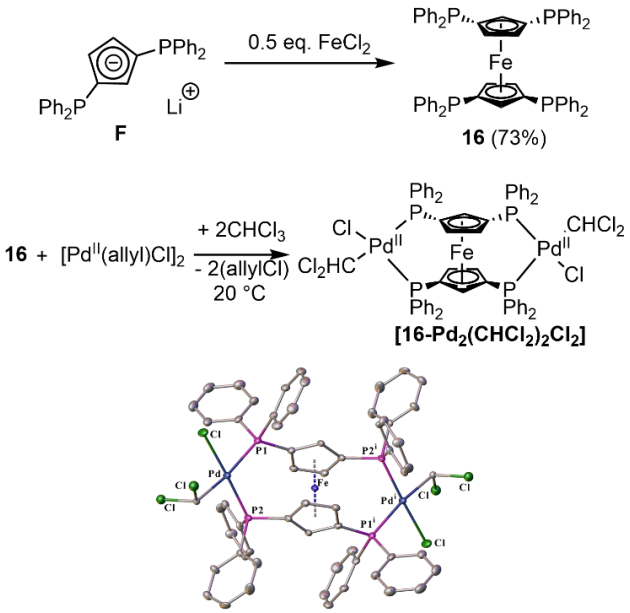

Figure 10. Synthesis and molecular structure of chloroform O.A. palladium complex of **16** [symmetry transformation: (i) 1-x, 1-y, -z].

Selective thioetherification of a large range of functionalized arene thiols was achieved with chloroheteroaromatic partners at the highest TONs up to 500 with Pd catalyst content down to 0.2 mol%.[42] A variety of reactive functions was tolerated with the coupling of thiophenols to six and five-membered 2-chloroheteroarenes, functionalized pyridine and pyrazine, quinoline, pyrimidine, furane, thiazole, and 3-bromoheteroarenes (pyridine and furane). Electron-rich congested thiophenols, as well as fluorinated thiophenols, were also suitable partners. The couplings of unprotected amino-2-chloropyridines with thiophenol, as well as the successful employment of synthetically valuable chlorothiophenols, were described with the same catalyst system. DFT studies conducted in cooperation with M. Saeys group attributed the high performance of this binuclear palladium catalyst to the reduced stability of thiolate-containing resting states.[42]

Some dissymmetric ferrocenyl phosphines have been synthesized by post-functionalization of preformed ferrocene derivatives, especially using directing groups on ferrocene like amine, acetal, sulfoxide, amide, oxazoline, *etc*.[4,43] However, to obtain rare 1,2- plus 1',3'-substituted ferrocenes, the assembling of two different functionalized Cp salts in a two-step protocol is necessary, and allows some very original dissymmetric tetraphosphine formation like for instance **17** that was obtained in 45% yield (Figure 11).[43] This synthetic way inspired the synthesis of many new ferrocenyl triphosphines obtained in good yields and exploited for various catalytic cross-couplings with palladium.

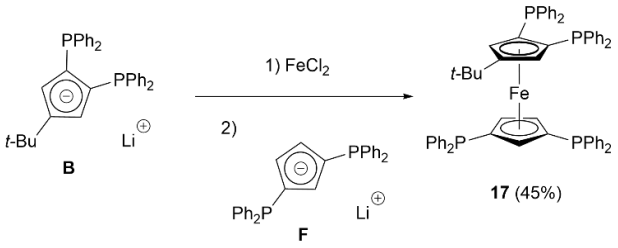

Figure 11. Synthesis of the dissymmetric 1,2,1',3'-tetrakis(diphenylphosphino) ferrocene **17**.

2.2. Triphosphines

The assembly of different functionalized cyclopentadienyl rings at $FeCl_2$ provides a robust method to access various ferrocenyl triphosphines with different electronic and steric properties at the donor atoms. It allows also the introduction of a variety of other structuring substituents on ferrocene backbone.

This synthetic method, however, preferentially leads to the formation of symmetric products, and as a consequence, limits the yields of dissymmetric (triphosphine) targets. Yet, in some cases satisfactory yields are reachable –the course of this selectivity remains an unpredictable experimental issue. Thus, the reaction of Cp ring **A** with iron dichloride, followed by the addition of **G** lead to the formation of **18** in 63% yield (Figure 12).[19] The coordination of **18** to $Cr(CO)_4$NBD gave complex **[18–Cr(CO)$_4$]** in 86% (Figure 13).[19]

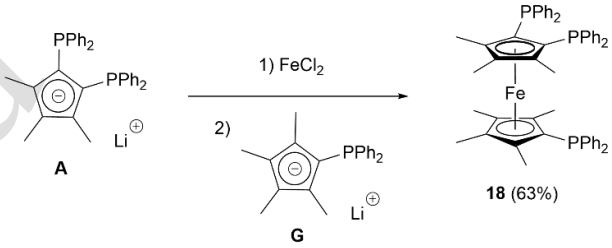

Figure 12. Synthesis of ferrocenyl triphosphine **18**.

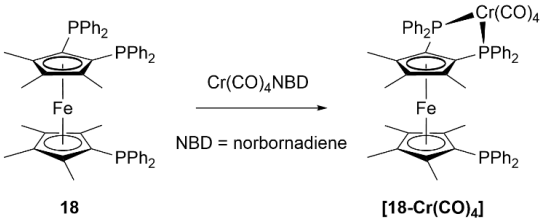

Figure 13. Coordination of **18** with $Cr(CO)_4$NBD.

The assembly synthetic route (Fig. 12) was successfully extended to a wide variety of ferrocenyl triphosphines (Figure 14). By reacting the precursor Cp **B** with various rings (Cp **H–R**) the formation of ferrocenyl triphosphines **19–29** was achieved.[43,44,46,47] Except for **19** and **20**, which have excellent yield (84% and 70%), and for **25** obtained with a satisfactory 55% yields, the other synthesis suffered from the selectivity limitation evoked above. Both the competitive formation of symmetric compounds and eventually tedious purification processes are responsible for these yields (3-35%). However, even with low yield, the access to these new class of ferrocenyl triphosphines is hardly achieved by post-functionalization of ferrocene.

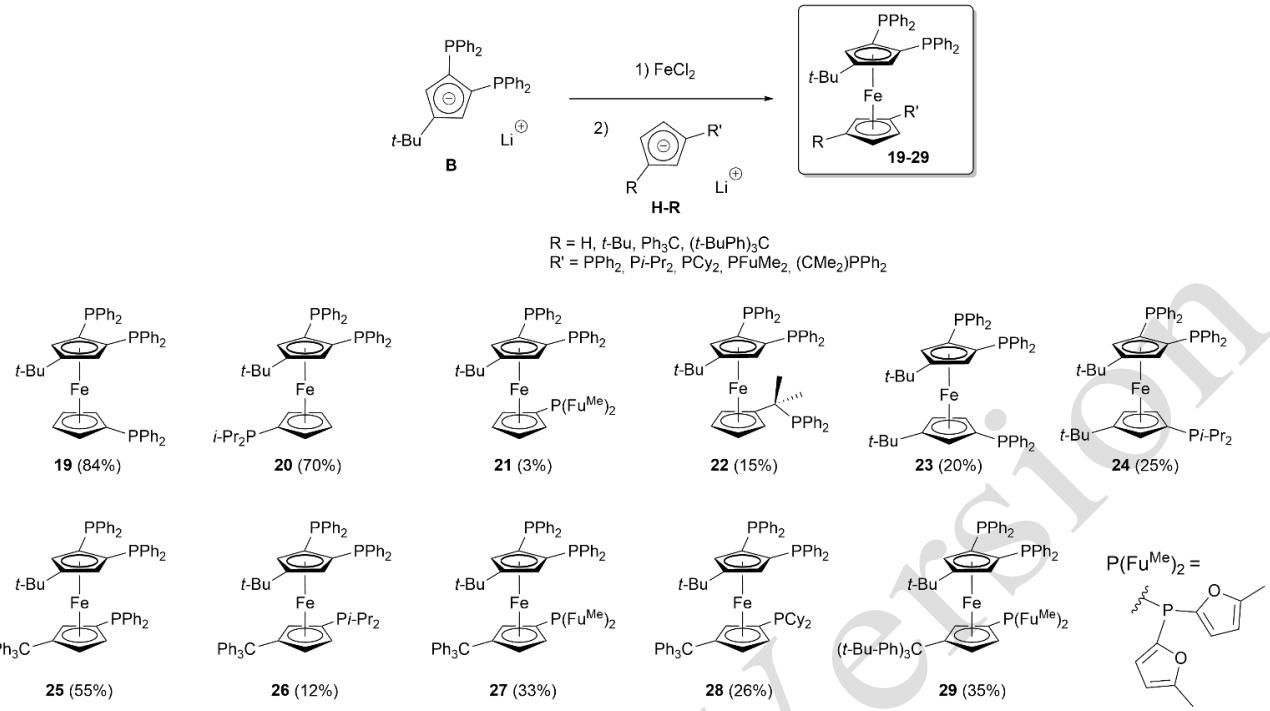

Figure 14. Synthesis of ferrocenyl triphosphines **19–29** by two Cp rings assembly at $FeCl_2$.

Depending on the conformation adopted in solution, these triphosphines can reveal close proximity between heteroannular phosphorous atoms as observed from strong ^{31}P NMR spin-spin coupling operating through-space *via* lone pair overlap ($^{TS}J_{PP}$) as observed for the ferrocenyl tetraphosphine **4** (Fig. 3).

Thus, ^{31}P NMR delivers information about the solvated conformation of these ferrocenes. For instance, while **20–22** did not show $^{TS}J_{PP}$ coupling, compound **19** displayed a $^{TS}J_{PP}$ coupling between the two vicinal phosphorus atoms and the heteroannular one (Figure 15, top). Consistently, this spin-spin coupling is strongly influenced by the solvent nature with a J_{PP} constant of 2.8 Hz in $CDCl_3$, and 5.0 Hz in C_6D_6.[43]

Whereas the different phosphorus donors in compound **20** showed no TS spin-spin coupling, a rarely exemplified through-space coupling $^{TS}J_{CP}$ = 5.5 Hz was observed between the heteroannular phosphorous atom and the three methyl carbon atoms of *t*-Bu substituent (Fig. 15, top). A spatial proximity has been confirmed in the solid state by XRD, with a short C···P distance of 3.64 Å.[43,48]

For these triphosphines the presence of a substituent on the monophosphinated Cp ring induces a loss of symmetry. Thereby, the two vicinal phosphorous atoms become anisochronous and their spin coupling is directly observable on the NMR spectrum. The ^{31}P NMR spectra results in various AB spin systems as observed in compound **23** and **24** ($^{3}J_{PP}$ = 98 and 87 Hz, respectively, Fig. 15). These two compounds do not present through-space coupling with the third heteroannular phosphorous atom. The analogues in which a ring substitution with a triphenylmethyl group is present (trityl, **25–29**) however display such ^{31}P–^{31}P spin-spin couplings. This TS coupling can occur with only one of the vicinal phosphorous atom as for **26** ($^{TS}J_{PP}$ = 6 Hz in $CDCl_3$, Fig. 15, bottom), or with both phosphorus donors as for **25** and **27–29**. The coupling constants can be either different ($^{TS}J_{PP}$ = 22 and 6 Hz for **28**), or similar (between 11 to 23 Hz for **25**, **27** and **29**) (Fig. 15, bottom), which gives an indication of the spatial proximity of the phosphorus atoms in solution and their mutual positioning.[46]

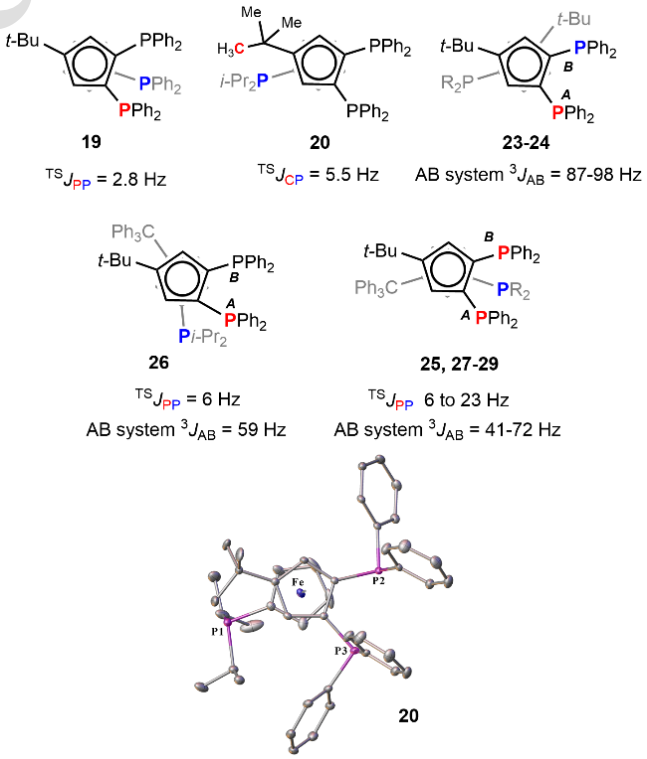

Figure 15. Average conformation of ferrocenyl triphosphines in $CDCl_3$ solution (view from above), according the existence and values of J_{PP} couplings.

Several of these triphosphines **19–29** have been studied in catalysis, in cooperation with H. Doucet group, and some

achieved remarkable performances in palladium-catalyzed cross-coupling reactions. The ferrocenyl triphosphines **19** and **20** with one non-alkylated Cp ring presented an excellent activity as ligands in Pd/Cu-catalyzed Sonogashira cross-coupling reactions. Compound **20** showed high robustness and activity giving TONs up to 250 000 for coupling phenylacetylene with bromoacetophenone (Figure 16, left).[15,41,47,49,50] The mixed ferrocenyl aryl/alkyl triphosphine **20** is thermally stable and insensitive to air or moisture, and its robustness allows aryl alkynylation at 10^{-1} to 10^{-4} mol% catalyst loadings, copper-free coupling using phenylacetylene is also accessible in good yield. Unconstrained triphosphine **19** has been used in the C–H bond activation of heteroarenes with TONs up to 9 000 for coupling (Fig. 16, middle).[51] The coupling of some sterically hindered bromoarenes to alkylated furans and thiophenes gave good to excellent yields using 0.1 mol% catalyst. Very high yields for coupling thiophene and 1,3-thiazole derivatives with activated bromides were achieved using only 0.1 to 0.01 mol% catalyst.[51] Compound **20** has presented a noticeable selectivity in C–N palladium-catalyzed bond formation for coupling of aniline derivatives to challenging difunctionalized dichloroarenes (Fig. 16, right).[52,53]

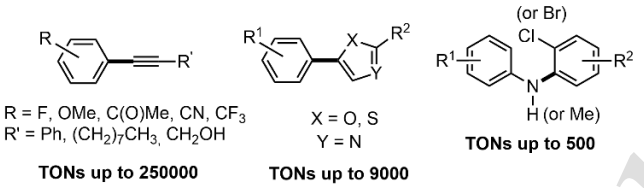

Figure 16. Sonogashira coupling, heteroarene C–H activation C–N bond formation promoted by non-congested ferrocenyl triphosphines.

Ferrocenyl triphosphines built from one unconstrained monofunctionalized Cp ring are useful ligands in the previous catalytic reactions, but they were found generally inactive in more challenging C–H functionalization reactions. However, the analogous five-functionalized triphosphines **23-25** –with a more constraint conformation– were found active in the use of demanding haloarenes such as aryl chlorides and congested aryl bromides. The ligands **23–25** associated with Pd have shown a very good activity for arylation of highly functionalized heteroaromatics with TONs up to 1 800 (Figure 17).[44,54,55] Thus, ligand **25** was mainly used for bromoarene substrates, but by using triphosphine **23**, electron-rich, electron-poor and multifunctionalized furans, thiophenes, pyrroles or thiazoles were arylated by various chloroarenes at 0.1-0.5 mol% catalyst loadings.

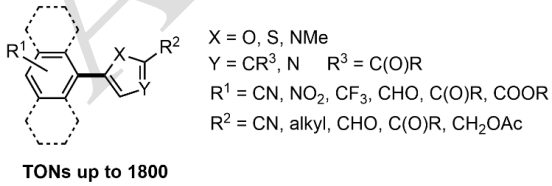

Figure 17. Arylation of heteroarenes by direct C–H activation promoted by constrained ferrocenyl triphosphines **23–25**.

Triphosphine ligand **24** associated with palladium promotes the coupling of hindered substrates such as 2-bromobiphenyl, 9-bromoanthracene and 2,6-dimethylbromobenzene to the same wide variety of heteroaromatics. These coupling reactions can generally again be performed by using catalyst low-loading ranging in 0.1-0.5 mol% Pd/ligand. Overall, Pd/triphosphine **23–25** catalytic systems generally tolerate useful functions such as formyl, nitriles, nitro, keto, and ester groups in *para*-, *meta*- or *ortho*-positions of aromatics.[55]

In addition to relevant performances in C–H bond functionalization, the triphosphine **24** also achieved unprecedented activity in palladium-catalyzed C–O bond formation *via* etherification of functionalized phenols with 2-chloroheteroarenes.[45] The air-stable palladium/triphosphine **24** system is efficient for the selective synthesis of heteroaryl aryl ether by using 0.2 mol% or less of catalyst. Thus, *para-, meta-* and *ortho*-substituted phenols with electron-donating or electron-withdrawing groups (including unprotected aminophenol) couple with a wide scope of heteroaryl 2-chlorides, including pyridines, pyrimidines and thiazoles bearing cyano, methoxy, and fluoro unprotected groups. This catalytic system was used in ten to fifty fold lesser amount of palladium and ligand than the previously reported systems, resulting in TONs up to 500 (Figure 18).[45]

DFT calculations conducted in M. Saeys group demonstrated that the conformation control in ferrocenyl triphosphine **24** open up new pathways for C–O reductive elimination, which do involve the third phosphine group (Figure 19). The rate for one of these new pathways was calculated to be about 10^3 times faster than for reductive elimination from a complex with a similar ferrocenyl ligand, but without phosphino group on the second cyclopentadienyl ring. The coordination of the third phosphino group to the Pd(II) center stabilizes the transition state in this new pathway, thereby enhancing the reductive elimination rate.[45]

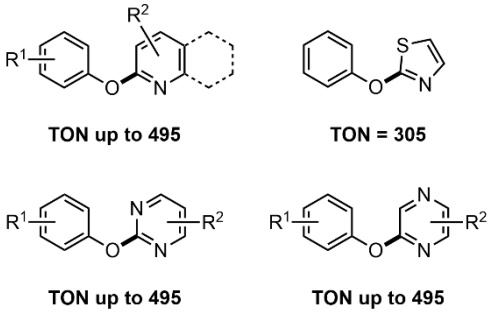

Figure 18. Palladium catalyzed etherification of functionalized phenols with chloroheteroarenes promoted by constrained ferrocenyl triphosphines **24**.

Reductive elimination (R.E.) is known to be the decisive step in aryl ether formation, and the bulkiness of air-sensitive electron-rich monophosphines has been reported to promote this reaction. We provided the first study of polydentate ligand influence in this reaction. As shown in Figure 19, relevant pathways involve isomerization between homoannular coordination (1,2-bonded, **iso.1** and **iso.4**, Fig. 19) and heteroannular (1,1'-bonded **iso.2** and **iso.3**, Fig. 19), reachable with a low barrier (E = 2 and 9 kJ.mol^{-1}). In **iso.3**, the free phosphorous from top Cp ring comes closer to the Pd(II) center forming a pseudo pentacoordinated palladium intermediate with a lower barrier (E = 83 kJ.mol^{-1} **RE.TS3**, Fig. 19, bottom). Faster reductive elimination may occur and the resulting Pd(0) complex formed is stabilized by a three-P donors coordination (–108 kJ.mol^{-1} **P**, Fig. 19, bottom).[45]

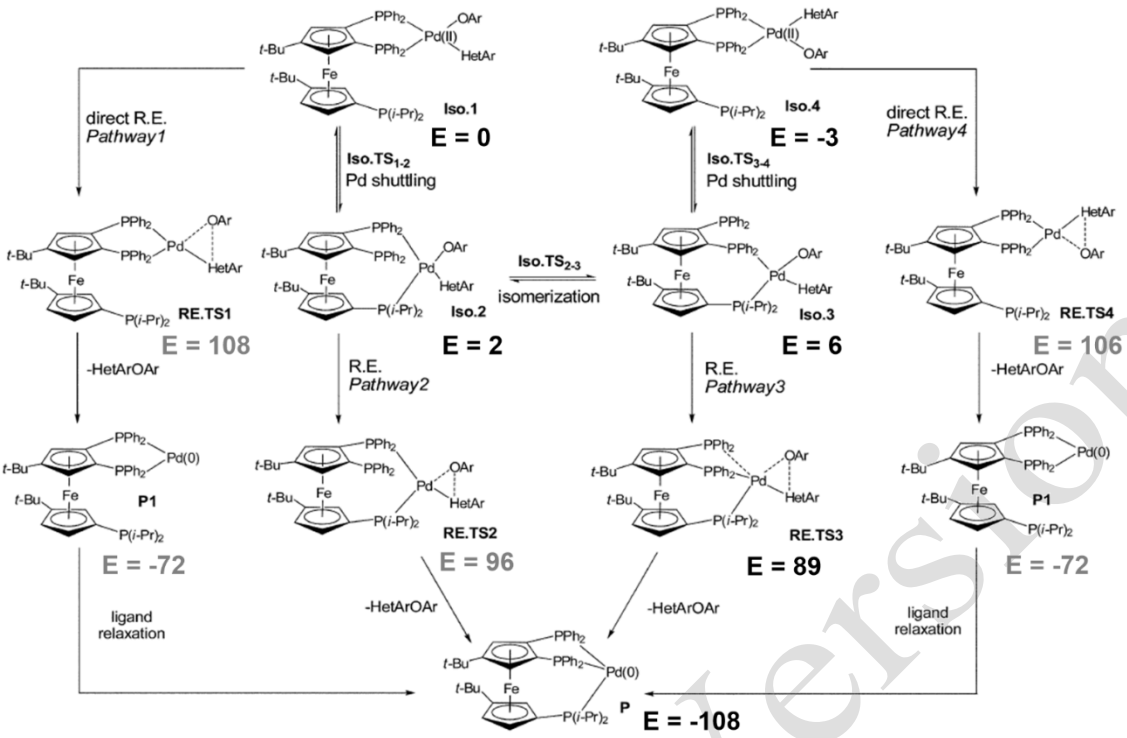

Figure 19. DFT calculation of reductive elimination pathway from **24-Pd(II)** complex (E in kJ.mol^{-1}).

Because of their efficiency in Pd-catalyzed C–C and C–O bond formation, ferrocenyl triphosphines were extended to specimens "ready for immobilization", as we achieved for a number of ferrocenyl tetraphosphines (Fig. 8). The triphosphines **30–35** (Figure 20) were obtained by the assembly of substituted cyclopentadienyl lithium at $FeCl_2$, using the same kind of precursors as **E** (Fig. 7), together with (phosphino)cyclopentadienyl lithium salts.[39,40]

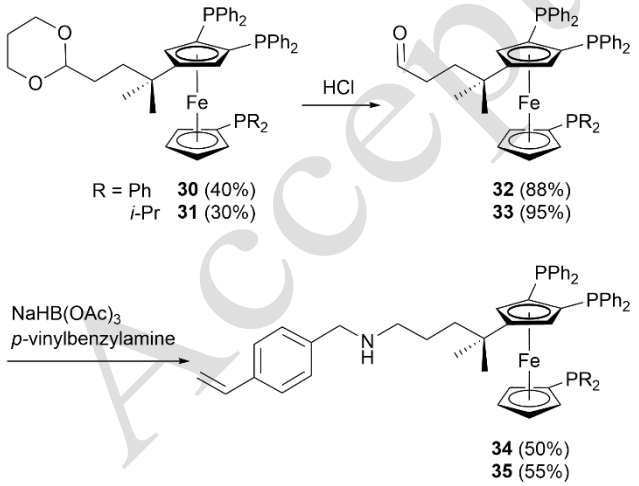

Figure 20. Tail-functionalized triphosphines **30-35** "ready for immobilization" on various supports.

In cooperation with P. Toy group, the functionalized triphosphine **35** was immobilized by radical-induced copolymerization with styrene (60 equiv) and divinyl benzene (7 equiv) to give an insoluble resin with a 1.05% phosphorus content.[40] This heterogenization strategy was applicable to the entire class of triphosphine ligands (and tetraphosphines), and which contain the 1,2-bis(diphenylphosphino)-4-*tert*-butylcyclopentadienyl fragment. The resulting polystyrene supported ligand **35–PS** has been engaged in palladium-catalyzed cross-coupling by direct C–H functionalization, and in copper-free Sonogashira coupling of bromobenzene with phenylacetylene (Figure 21).[40] In general, the resulting cumulative turnover numbers, TONs ranging 270–1700, of the catalysts were satisfactory relative to their homogeneous counterparts when used with chloroarenes, and showed good potential for recycling. The unsupported analogues yielded TONs over 10^4 with bromides under homogeneous conditions, which was not reached by the supported ligands to date. Indeed, efficient recycling of the catalysts after six runs cannot be established because of accumulative loss of material during filtration. Overall, we described an efficient strategy for assembling a new class of branched tetra- and triphosphine ligands with a unique rigid conformation of ferrocene providing a high local density of phosphorus atoms for an extended coordination to the metal center. This study provided proof-of-concepts of supported catalytic materials built from modular polyphosphines to generate polydentate heterogeneous catalysts both active for C–C cross-coupling reactions and even very challenging C–H functionalization from chloroarenes.

Figure 21. Polystyrene supported **35–PS** in palladium catalyzed arylation of heteroarene and Sonogashira coupling.

While highly functionalized ferrocenyl polyphosphines present unique properties, their synthesis mode also encouraged us to develop simpler, more easily accessible ferrocenyl diphosphines. Still the search for conformation control and pertinent ring

additional modifications ultimately led to the development of different classes of tetrasubstituted ferrocenyl diphosphines.

2.3. Diphosphines – 1,1'-diphosphine alkylated symmetric specimens

The direct functionalization of the ferrocene backbone most generally enables the synthesis of two big families of diphosphines, which can be distinguished as either 1,1'-homoannular and 1,2-heteroannular diphosphines, depending on the place of the phosphorus atoms substitution on the Cp rings.

The commonly developed 1,1'-homoannular ferrocenyl diphosphines bear two identical phosphino groups on each ring (dppf is the typical example). Compound **36** was the first specimen of highly functionalized symmetric ferrocenyl diphosphines which was synthesized in Dijon laboratories in the 1990s.[56] This ferrocene derivative was obtained in moderate yield (46%) by reacting the tetramethylated (diphenyl)phosphino Cp ring **G** with $FeCl_2$ (Figure 22).[57]

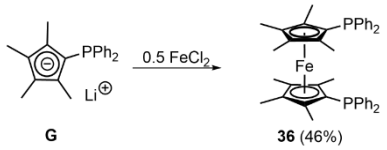

Figure 22. Synthesis of diphosphine **36**.

The phosphine oxide derived from **36** has shown good activity as phase-transfer catalyst in nucleophilic substitution reactions of alkyl halides with potassium iodide or thiocyanate.[58] The complexation of **36** with groups 6 and 7 transition metals Cr, Mo, W, and Mn displayed a variety of monoligate and bridging or chelating biligate coordination (Figure 23).[58]

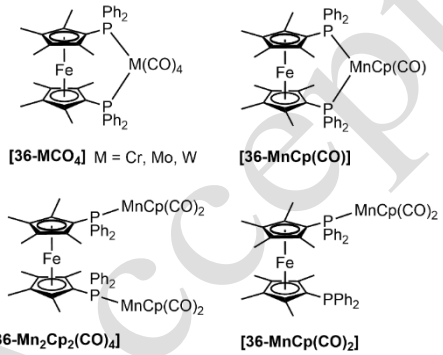

Figure 23. Different coordination modes of diphosphine **36**.

However, the synthesis of the precursor Cp ring **G**, was found tedious and therefore dialkylated ferrocenyl diphosphines were developed by our group following this pioneering work.

To produce 1,1'-heteroannular diphosphines with dialkylated ferrocene backbone two synthetic pathways are accessible, which are distinguished as “converging” and “diverging” pathway (Figure 24). The converging way is illustrated by the assembly synthesis of **36**, while the diverging way is based on the post-functionalization of a preexisting dialkyl ferrocene. The presence in 1,3-position of two substituents on each Cp ring induces the formation of two diastereoisomers, a chiral compound in racemic mixture (*rac*) and the achiral *meso* stereoisomer (Figure 24).

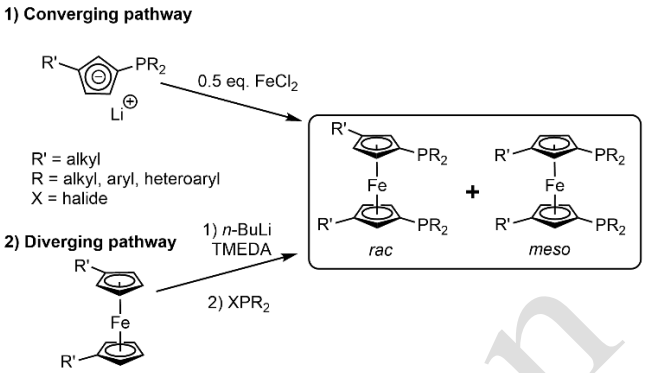

Figure 24. Synthetic access to alkylated 1,1'-heteroannular ferrocenyl diphosphines.

Bis(phosphino)ferrocenes **37**–**39**, bearing bulky groups such as *tert*-butyl and –OSi(*i*-Pr)$_3$ on the Cp rings were obtained using a converging method (Figure 25). The assembling of Cp salts **L**, **M**, and **S** provided the expected mixture of *rac* and *meso* diastereoisomers.[31,44,57] Diastereomers **37** and **37'** were separated by column chromatography, while **38** and **39** could not be easily separated from achiral **38'** and **39'**, respectively.

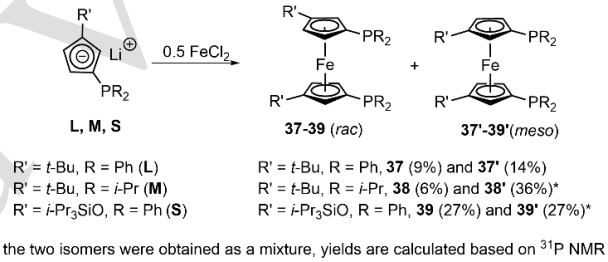

* the two isomers were obtained as a mixture, yields are calculated based on ^{31}P NMR

Figure 25. Synthesis of ferrocenyl diphosphine **37–39** by cyclopentadienyl (Cp) rings assembling method. Pure rac isomers synthesis (see below) and XRD allowed the identification of stereoisomers.[31,44,57]

Ferrocenyl diphosphines **40'**–**42'** bearing a (triphenyl)methyl group (trityl) on Cp rings were also synthesized by the converging way.[46] The trityl group on Cp rings decreases the global nucleophilicity of the ring and generates a significant steric hindrance. For an unclear reason, probably related to the hindrance of trityl groups, compounds **40'** and **41'** were obtained as a single *meso* diastereoisomer, while the mixture **42** and **42'** was not resolved (Figure 26).

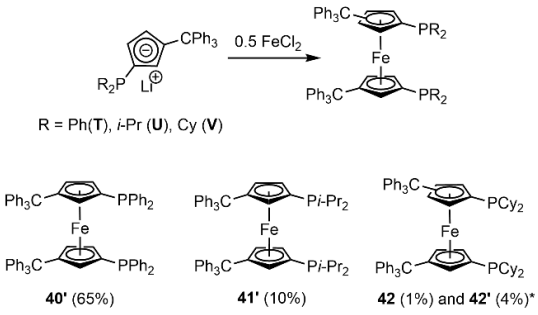

*the two isomers were obtained as a mixture, yields are calculated based on ^{31}P NMR

Figure 26. Ditrityl substituted ferrocenyl diphosphines.[46]

The complexation of **40'** with [PdCl-(η_3-C_3H_5)]$_2$ produced **[40'–Pd(allyl)Cl]** in quantitative yield (Figure 27).[46] The ^{31}P variable-

temperature NMR (VT-NMR) experiment of **[40'–Pd(allyl)Cl]** in CD_2Cl_2 showed at 298 K (25°C) two overlapping singlets located at 21.1 and 21.5 ppm. Upon heating at 318 K (45°C), these two singlets coalesce into a singlet at 21.3 ppm attributed to the rapid dynamic exchange between the anisochronous phosphorus. Upon cooling to 278 K (–20°C), the exchange phenomenon slowed down, resulting in an AB spin system centered at 21.2 ppm with a J_{AB} = 46 Hz. This dynamic behavior remind the fluxionality also observed in the tetraphosphine ferrocenes (Fig. 5), showing the relationship between these ferrocenyl phosphine metal/allyl derivatives.

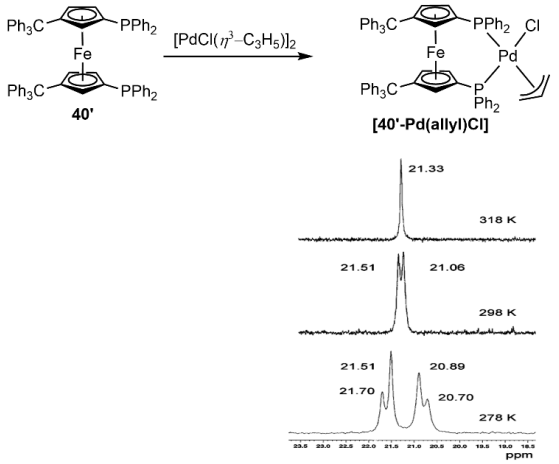

Figure 27. Complexation of **40'** with palladium and ^{31}P VT–NMR (CD_2Cl_2) experiments.

The ferrocenes **40'**–**42'** were tested in the palladium-catalyzed arylation of aromatic heterocycles *via* C–H bond activation (Figure 28).[44,46] The palladium complex of the diphosphine **40'** was successfully used in the direct C–H activation of electron-rich heteroaromatics for coupling to demanding aryl bromides, whether electron rich and/or sterically congested. Products such as 2-butyl-5-(4-methoxyphenyl)furan, 2-butyl-5-*o*-tolylfuran, and thiophene analogues were obtained in yields higher than 90%.[32] We further demonstrated the higher performance of the electron-rich diphosphines **41'** and **42/42'** (in diasteromeric mixture) in the arylation of substituted furans with functionalized electron-deficient aryl chlorides, such as 4-chlorobenzonitrile, 4-chloronitrobenzene, 4-chloropropiophenone, and 4-(trifluoromethyl)chlorobenzene. The performances illustrate the utility of air-stable, moisture-insensitive alkylated electron-rich diphosphines in this specific arylation reaction. We assumed by comparison with other ferrocenyl di- and triphosphines that these ligands promote oxidative addition, because of electron-rich alkylated-P donors and that the large bite angle that is associated to 1,1'-phosphorus-chelating coordination may facilitate reductive elimination at palladium.

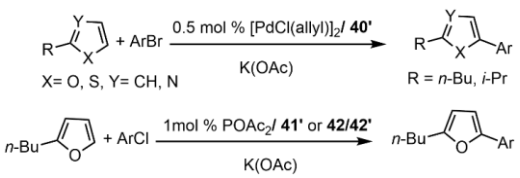

Figure 28. Pd-catalyzed C–H arylation of heteroaromatics with bromo and chloroarenes using diphosphine ligands **40'**, **41'**, **42/42'**

We were pleased to recently achieve the diastereoselective synthesis of a new series of dialkylated ferrocenyl diphosphines bearing aryl, alkyl and hetero- or polycyclic substituents on the phosphorus atom (Figure 29).[59] The diverging synthetic route was beneficially employed and was unexpectedly selective. Apparently, the steric effect of the substituents present on the ferrocene platform has a significant influence on the stereoselectivity during the lithiation (with a presumed joint structuring role of *tert*-butyl and TMEDA) and phosphination steps. The *tert*-butylated ferrocenyl diphosphines **37**, **38** and **44**–**47** were synthesized as pure *rac* stereoisomer in good to excellent yields (42-88%, Fig. 29) from the alkylated precursor **43a**.

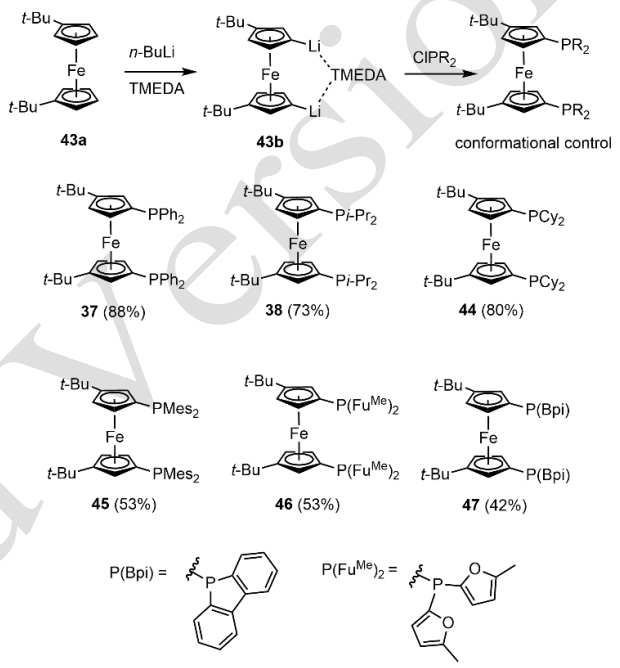

Figure 29. Diastereoselective synthesis of ferrocenyl diphosphines **37**, **38** and **44**–**47** by sequential lithiation/phosphination of dialkylated ferrocene.

For compounds **37** and **38** the converging synthetic pathway gave the mixture of *rac* + *meso* diastereoisomers in moderate to low yield (23-42%, Fig. 25), but these phosphines are obtained as pure *rac* diastereoisomers in much higher yield of 88% and 73%, respectively, from a lithiation/phosphination sequence (Fig. 29). Compounds **44**–**47** are obtained in satisfactory yield despite the low stability of some of the corresponding phosphination agents under the reaction conditions. Thus, the post-functionalization of the *tert*-butylated ferrocene platform constitutes a powerful strategy for the diastereoselective synthesis of symmetrically substituted 1,1'-diphosphines. Accordingly, the analogous compounds holding *i*-Pr groups, **50** and **51**, and trimethylsilyl (TMS), **52** and **53,** have also been synthesized from ferrocene post-functionalization (Figure 30).[59,60] Compounds **50** and **51** were synthesized from precursor **48a** in two steps, and **52** and **53** obtained in a one-pot protocol from **49a**, without isolating the intermediate **49b** (35% and 33% overall yields, respectively). The introduction of less congested *i*-Pr group on the ferrocene platform decreases the diastereoselectivity of the reaction leading to the formation of a diasteroisomeric mixture of **51** and **51'**, confirming the unique role of *tert*-butyl groups.

The bis(phosphino)ferrocenes **37**, **38** and their analogs **44**–**47** and **50**–**53** were all tested in the substitutive nucleophilic fluorination of 2-chloroquinoline and chloropyridine derivatives using mild palladium-catalyzed conditions.

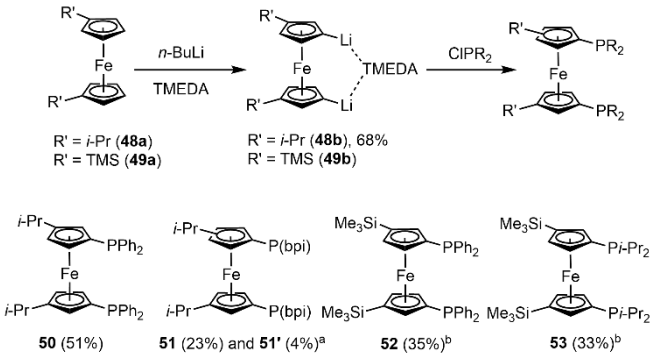

[a] the two isomers were obtained as a mixture, yields are calculated based on ^{31}P NMR
[b] overall yields

Figure 30. Alkylated diphosphines **50–53** holding *i*-Pr and TMS groups.

Among these diphosphines, **37** (Fig. 29) is the most effective for assisting transhalogenation by using AgF as nucleophilic F^- source. However, to our surprise the complete removal of palladium in the reaction much reduces detrimental side reactions such as dehalogenation and homocoupling, and also avoids the facile fluorination of the phosphorus atoms (δ^{31}P 45.12, and δ^{19}F –73.29 ppm, with $^1J_{P,F}$ = 1020 Hz). Finally using palladium-free conditions with bis(phosphino)ferrocenes clearly assured, in our hands, a better reproducibility of fluorination. This nucleophilic transhalogenation albeit of limited scope avoided strictly anhydrous conditions and the use of highly specialized fluorination reagents.[59]

The complexation of some of these 1,1'-diphosphines with gold(I) halide were studied, in view of further extension to gold-catalyzed reactions related to dinuclear species and the promotion of a better control in generating Au···Au aurophilic interactions. *tert*-Butylated diphosphines *meso* **37'** and *rac* **46** (Fig. 25 and 29) were reacted with two equivalents of [AuCl(SMe)$_2$] quantitatively yielding dinuclear gold (I) species **[37'–Au$_2$Cl$_2$]** and **[46–Au$_2$Cl$_2$]**, respectively (Figure 31).[31] Based on XRD structure in the solid state and ^{31}P NMR in solution at –80°C complex **[37'–Au$_2$Cl$_2$]** formed the expected dinuclear complex with an intramolecular aurophilic interaction Au···Au' showing a $d_{Au\cdots Au'}$ = 3.0781(6) Å. An aurophilic interaction was also observed in **[46–Au$_2$Cl$_2$]** with a distance Au···Au' slightly longer $d_{Au\cdots Au'}$ = 3.2349(6) Å (Fig. 31).[31] Compared to dppf, the introduction of *tert*-butyl groups induces a smart steric control of the metallocene backbone in bis(phosphino)ferrocene ligands which favors intramolecular aurophilic interactions between [AuCl] fragments in dinuclear gold(I) complexes.

The complexation of the diastereomeric mixture of **39**/**39'** with two equivalents of [AuClSMe$_2$] provided in 1:1 ratio the corresponding complexes **[39–Au$_2$Cl$_2$]** and **[39'–Au$_2$Cl$_2$]**. The complex **[39–Au$_2$Cl$_2$]**, from *rac* **39**, crystallized independently, and could be isolated pure in 40% yield. The XRD analysis shows that it belongs to the C2-symmetry point group. The orientation of the phosphino groups displays a large torsion angle that precludes short contact distances and induces gold centers separation above 6.0 Å (Fig. 31). Unlike *tert*-butyl groups, lesser steric control exerted by −OSi(*i*-Pr)$_3$ groups was attributed to the oxygen atom, seen as a spacer, which presumably add a rotational degree of freedom to the ferrocene platform. Current studies of these dinuclear gold complexes aim at their use in catalytic reactions including C–C bond formation by cross-coupling and enynes cycloaddition.

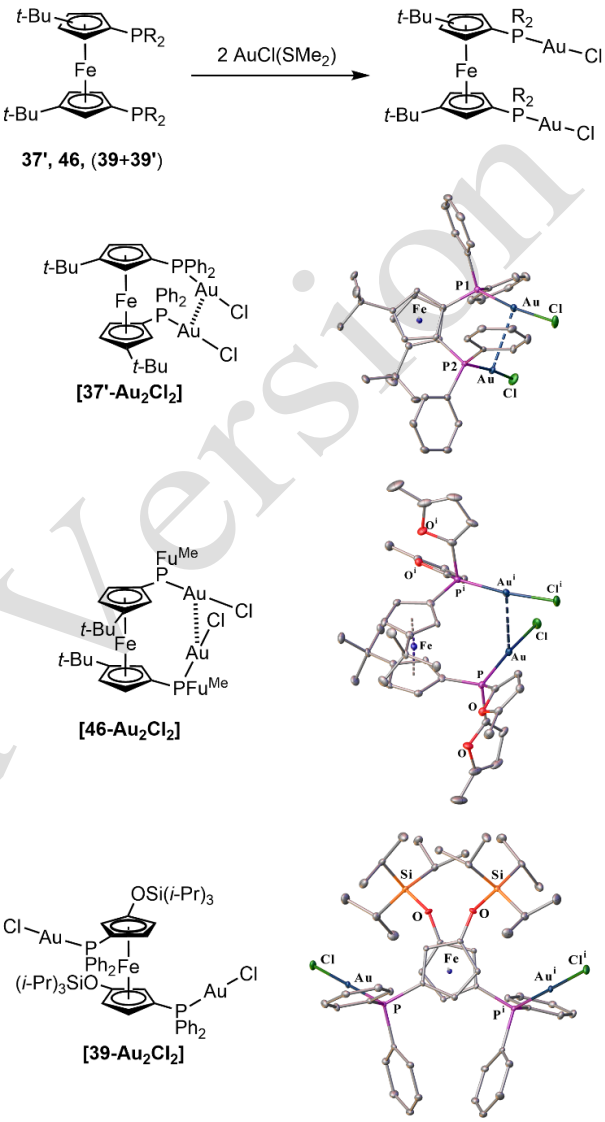

Figure 31. Dinuclear gold(I) chloride bis(phosphino)ferrocene complexes illustrating aurophilic and non-aurophilic situations (ORTEP views, right) [symmetry transformations: (i) -x, +y, 3/2-z (**[46–Au$_2$Cl$_2$]**) and 1-x, +y, 1/2-z (**[39–Au$_2$Cl$_2$]**)].

2.4 Diphosphines – 1,1'-dissymetrically substituted specimens

For producing dissymmetric 1,1'-diphosphino substituted ferrocene derivatives the direct phosphination of the ferrocenyl backbone can be employed *via* opening of ferrocenophane **54b** (Figure 32). Our group reported the synthesis of unconstrained dissymmetric ferrocenyl diphosphine **55**, which bears both the electron-rich –PPh$_2$ and electron-poor –P(Fu^{Me})$_2$ groups.[61] Compound **55** was obtained in a modest 25% yield from **54c** (Fig. 32) because its hydrolysis product mostly formed (40%). Upon complexation to transition metals such compounds are expected to display some hemilabile behavior with possible

beneficial effects in catalytic reactions. Thus, the complex **[55–$PdCl_2$]**, obtained from the reaction of **55** and $PdCl_2(PhCN)_2$, was engaged in palladium catalyzed allylic amination.[61] In the presence of a low concentration of this complex as catalyst, used at 0.01 mol%, the coupling of aniline to allyl acetate occurs at a TOF (turnover frequency) of *ca* 5000 h^{-1}. Allyl amines were produced in good to high yields (75 to 99%) and excellent linear/branched selectivity (94/6%) when applicable, with for instance hex-2-en-1-yl acetate reacted with piperidine and morpholine. The addition of the less nucleophilic morpholine to allyl acetate was achieved with a TOF of 3330 h^{-1}. The amination of the sterically demanding geranyl acetate, a monoterpene derivative of interest in the flavor industry demonstrated the scope of this methodology, which provided noticeable advantages in terms of sustainable chemistry with high selectivity, and low metal content reactions.[61]

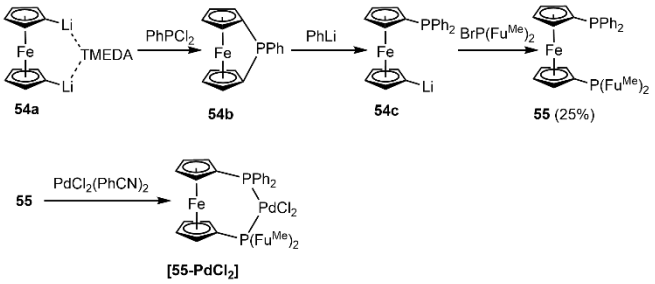

Figure 32. Hybrid diphosphine **55** and its complexation to $PdCl_2$.

A similar sequential functionalization starting from alkylated **43a** (Fig. 29) led to the formation of the hemilabile constrained ferrocenyl diphosphine **58** (Figure 33), which incorporates both –PPh_2 and –P*i*-Pr_2 groups.[62] Sequential ferrocene lithiation/bromination allowed the formation of brominated precursor **56** that is followed by two sequential distinct phosphinations. At larger scale (30 mmol instead of 1 mmol) both the monobromination and hydrolysis side products of **43a** were difficult to separate from **56** by standard chromatography methods. We developed with D. Lucas and C. Devillers group an innovative oxidative purification based on controlled electrolysis. The distinct redox potential of these three ferrocene derivatives allowed the selective oxidation of the two undesired side products, and the aqueous phase extraction of the formed ferrocenium species. This led to isolate **56** as a pivotal precursor for further functionalization in high purity at multigram scale (> 20 g).[62,63]

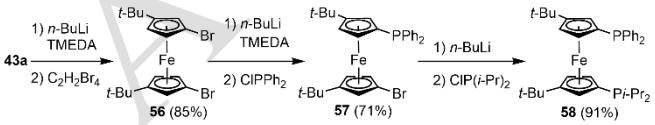

Figure 33. Synthetic pathway of hemilabile ferrocenyl diphosphine **58**.

2.5 Diphosphines –1,2-diphosphines alkylated specimens

By converging assembly of pre-synthesized 1,2-phosphinated Cp rings, the alkylated ferrocenes **59–61** could be prepared albeit in contrasted yields (Fig. 34). Compounds **59** and **60** were early on reported to be obtained in yields around 70%,[19,57] while in our hands decomposition and/or oligomerization of *in situ* formed formyl precursor gave a limited 20% yield of **61** (Figure 34).[31] However, the reactivity of the aldehyde group on the bottom Cp ring gives opportunity for further developing derivatives based on ferrocenyl 1,2-diphosphine structures.

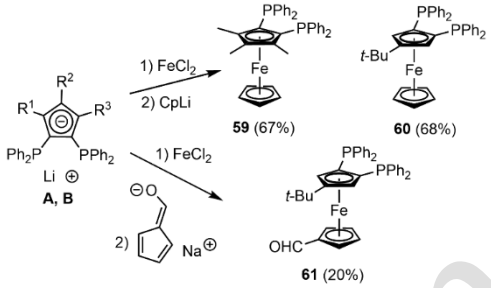

Figure 34. Synthesis of homoannular ferrocenyl diphosphines **59**–**61**.

The coordination of 1,2-diphosphine **59** with metal carbonyl complexes $M(CO)_4L_2$ (M = Cr, W and L = norbornadiene or piperidine) gave the corresponding group 6 transition metal complexes in excellent yield **[59–$W(CO)_4$]** and **[59–$Cr(CO)_4$]** (Figure 35).[19]

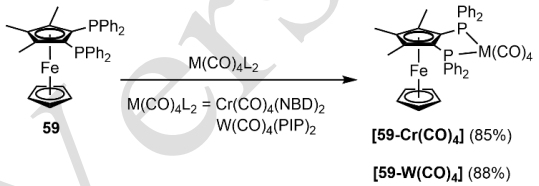

Figure 35. Complexation of **59** with group 6 transition metals.

The coordination chemistry of 1,2-diphosphine **60** with palladium and rhodium was studied (Figure 36). Palladium complex **[60–$PdCl_2$]** was obtained by the reaction of **60** with $(PhCN)_2PdCl_2$ and its catalytic reactivity was investigated in palladium-catalyzed olefin methoxycarbonylation and Heck C–C coupling.[65]

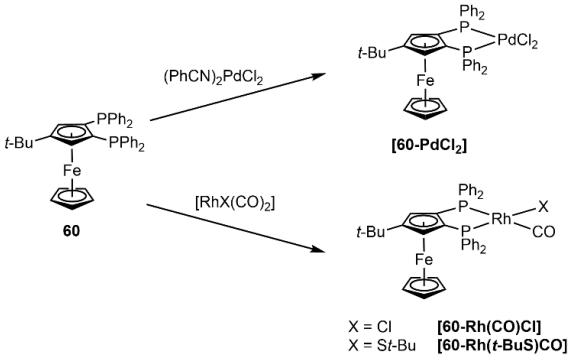

Figure 36. Complexation of **60** with rhodium and palladium

A variety of coordination schemes were obtained in the complexation of **60** with rhodium. The S-bridged dinuclear complex $[Rh(t\text{-BuS})(CO)_2]_2$ reacted with the ferrocenyl diphosphine **60** did not conserve the usual dinuclear framework and provided a mononuclear compound **[60–Rh(*t*-BuS)CO]**. The complex **[60–Rh(CO)Cl]** was formed from the reaction of **60** with $[RhCl(CO)_2]_2$ under CO atmosphere. In the absence of CO partial pressure, the reaction between **60** and the Rh precursor lead to the additional formation of cationic rhodium complex in *cis* and *trans* isomers mixture **62a** and **62b** (Figure 37). These cationic species were isolated from **[60–Rh(CO)Cl]** by precipitation, with $[RhCl_2(CO)_2]^-$ as counter ion. Complexes **62c** and **62d** were also obtained with chloride counter ions, by the

addition of an excess of ferrocenyl diphosphine **60** to the rhodium precursor $[RhCl(CO)_2]_2$.[65]

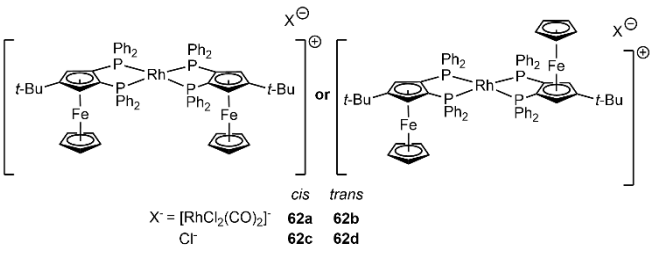

Figure 37. Cationic rhodium complexes **62a–d**.

Rhodium complexes **[60–RhCl(CO)]** and **[60–Rh(*t*-BuS)CO]** were employed in the catalytic hydroformylation of oct-1-ene, with a yield of aldehydes up to 96%.[65]

3. Ferrocenyl Amines and (P, N)-Hybrids

Based on the impetus provided by dialkylated tetraphosphines with a controlled conformation at the ferrocene platform, we developed the synthesis of polydentate aminomethyl ferrocenes and amino-phosphino ferrocenes also bearing *tert*-butyl groups on each Cp. We first explored a converging way by cyclopentadienyl assembly, but the stereoselectivity control and the mixture of diastereomers formed needed too long separation procedure and limited the yield. We consequently explored a diverging way to obtain these ferrocenes with a high diastereoselectivity.[66] This approach was initiated with the formation of aminomethyl and iminomethyl ferrocene derivatives.

3.1. *tert*-Butylated aminomethyl ferrocenes and iminomethyl ferrocenes ligands

The targeted *tert*-butylated aminomethyl ferrocene N-ligands were distinguished as secondary and tertiary amine derivatives (Figure 38).

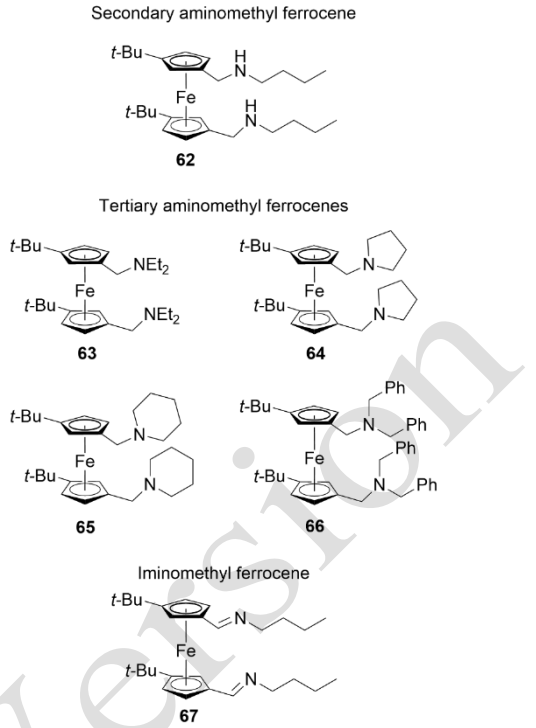

Figure 38. *tert*-Butylated amino and iminomethyl ferrocenes.

The secondary and tertiary aminomethyl ferrocenes **62**-**66** bear alkyl groups on each nitrogen atom. Compounds **62**, **63** and **66** includes acyclic alkyl groups of different steric size at nitrogen with ethyl, butyl and benzyl groups, and diamines **64** and **65**, hold cycloalkyl groups. The iminomethylferrocene **67** bears a long-chain butyl group. These ferrocene derivatives were synthetized by reductive amination from the diformylferrocene **68**, obtained in two steps from **43a** with a full diastereoselectivity confirmed by XRD (Figure 39). After lithiation and formylation of **43a**, the resulting compound **68** was reacted with primary or secondary amines and reduced using $NaHB(OAc)_3$, which allowed the selective formation of diamines **63**–**66** in very good to high yields (74-96%).[66] As for the synthesis of diphosphinoferrocenes presented before, this functionalization way offers a high diastereoselectivity with the exclusive formation of *rac* stereoisomers.

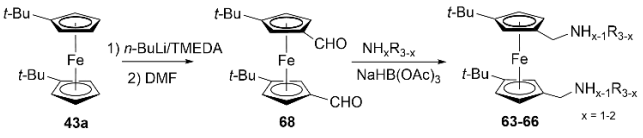

Figure 39. Synthesis of *tert*-butylated aminomethyl ferrocene derivatives.

The synthesis of secondary aminomethylferrocene **62** is similar to **63–66** however, with the use of 3/1 ratio of amine/aldehyde (Figure 40). $LiAlH_4$ was used for reducing the iminomethyl ferrocene **67**, leading to the secondary amine **62** with a high yield of 95%.[66]

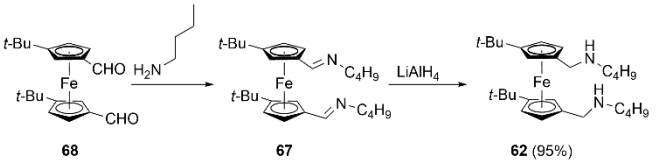

Figure 40. Synthesis of a *tert*-butylated secondary aminomethyl *via* an iminomethyl ferrocene.

A direct consequence of the introduction of *t*-Bu groups on the ferrocene platform was obtained by the coordination chemistry of **63** to $[PdCl_2(PhCN)_2]$ (Figure 41).[66] The spontaneous formation of a zwitterionic cyclopalladate **69** from C–H activation and nitrogen attack to form ammonium was observed that does not occur with analogue non-*tert*-butylated diaminoferrocenes. Zwitterionic cyclopalladate formation from an (aminomethyl)ferrocene derivative, arising from intramolecular Cp-proton transfer to the proximate free amino group by simple C−H activation reaction in the presence of palladium dichloride was unprecedented. This reactivity was attributed both to electronic effects and steric control of *tert*-butyl groups. The flexibility of nitrogen arm at the bottom Cp rings probably also allows this cyclopalladate easy formation.

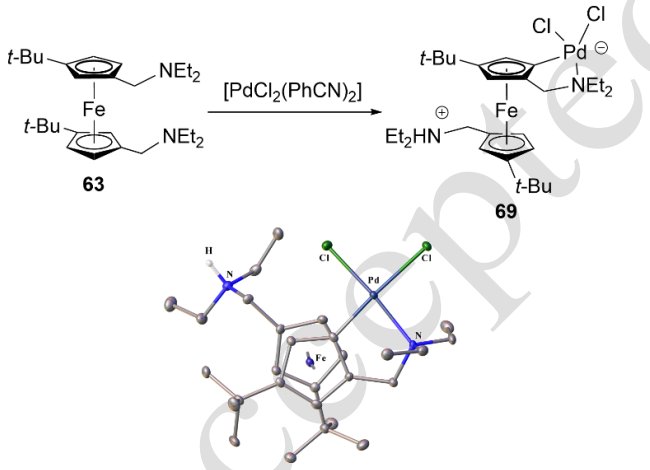

Figure 41. Intramolecular cyclopalladation of the diamine **63**.

From these *tert*-butylated aminomethyl ferrocenes, the synthesis of *tert*-butylated amino phosphino ferrocenes ligands by a post-functionalization strategy could be efficiently achieved.

3.2. *tert*-Butylated (N)-amino-(P)-phosphino ferrocene ligands

The synthesis of *tert*-butylated diamino diphosphino ferrocene ligands was attractive because of the possibility of coordination of both phosphorus and nitrogen atoms with transition metals. Therefore, the « soft » group (phosphine) and the « hard » group (amine) could be used as hemilabile system in catalytic reactions.[67] The various acyclic (**70–73**) and cyclic (**74**) amino groups we originally introduced, were complemented with a panel of phosphino groups bearing either electron-donating or electron-withdrawing groups of various steric hindrance (Figure 42, **71–74**).

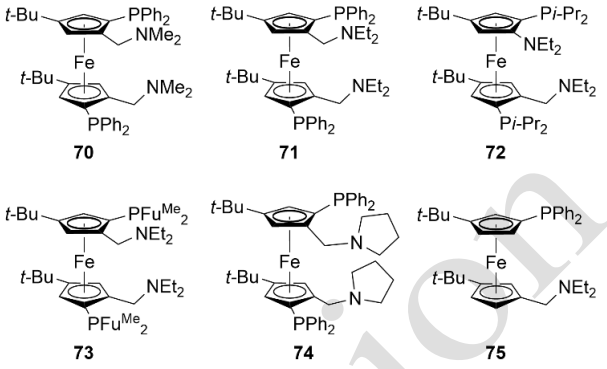

Figure 42. *tert*-butylated *N*-amino-*P*-phosphino ferrocenes.

Initially, the assembly of adequately substituted Cp salts was investigated for the formation of alkylated ferrocene (P,N)-ligands (Figure 43).[66] Dimethylaminomethylation of (diphenylphosphino)-3-*tert*-butylcyclopentadienyllithium **L** was achieved in a 86% yield using an iminium salt. The synthesis of the ferrocenes **70/70'** was achieved as a 2:1 mixture of *rac* and *meso* stereoisomers (39 % overall yields, that crystallized separately and were characterized by XRD and NMR, Fig. 43).[66] In this converging pathway the cyclopentadienyl phosphination precedes its amination. In the diverging way the amination of ferrocene allows directing *ortho*-lithiation followed by site selective phosphination of the platform, giving for **63** and **64** *rac* diastereomer with generally satisfactory yields (**71–74**, Fig. 43). The ^{15}N NMR measurement of ligands **70–74** indicates no significant interaction in solution between phosphorus and nitrogen atoms despite the relative proximity of these nuclei. *tert*-Butylated *N*-amino-*P*-phosphino ferrocene **75** (Fig. 42) has been synthesized by the introduction of the phosphino group in a first step, followed by 1'-formylation and reductive amination to obtain the hybrid compound **75** in 70% yield.[62]

The complexation of ligands **71**, **72** and **74** with palladium and gold was reported. The palladium complexation with bis(benzonitrile)palladium(II) chloride unexpectedly showed clearly distinct coordination modes depending on the palladium/ligand ratio and the ligand used.[62,68] With **71**, when one equivalent of Pd(II) was added, the flexibility of the ferrocene platform allows a 1,1'-(P,P)-heteroannular coordination by the chelating diphosphine (**[71–PdCl$_2$]**, Figure 44). Conversely, the use of two equivalents of palladium systematically led to the quantitative formation of a dinuclear palladium compound with bis-1,2-(P,N)-homoannular coordination: **[71–Pd$_2$Cl$_4$]**, **[72–Pd$_2$Cl$_4$]** and **[74–Pd$_2$Cl$_4$]**. Conversely, similar attempts to form the mononuclear palladium species from **72** and **74** led to mixture of complexes.

Complexation of **71**, **72** and **74** using chloro(dimethylsulfide)gold(I) led to the formation of dinuclear gold complexes **[71–Au$_2$Cl$_2$]**, **[72–Au$_2$Cl$_2$]** and **[74–Au$_2$Cl$_2$]** (Figure 45).[63] These were all characterized by a single ^{31}P NMR signal, which indicated a symmetric coordination mode involving phosphorus. FT-IR analyses of these complexes revealed the expected absorption bands between 321 cm^{-1} and 333 cm^{-1} and

the XRD structure of **[72–Au_2Cl_2]** confirmed a dinuclear gold(I) chloride linear coordination involving exclusively –P(*i*-Pr)$_2$ groups. For the ligand **71**, one equivalent of gold precursor was used in an attempt to obtain a mononuclear complex, but this reaction only led to a 1:1 mixture of the dinuclear complex together with the uncoordinated diaminodiphosphino ferrocene.[69]

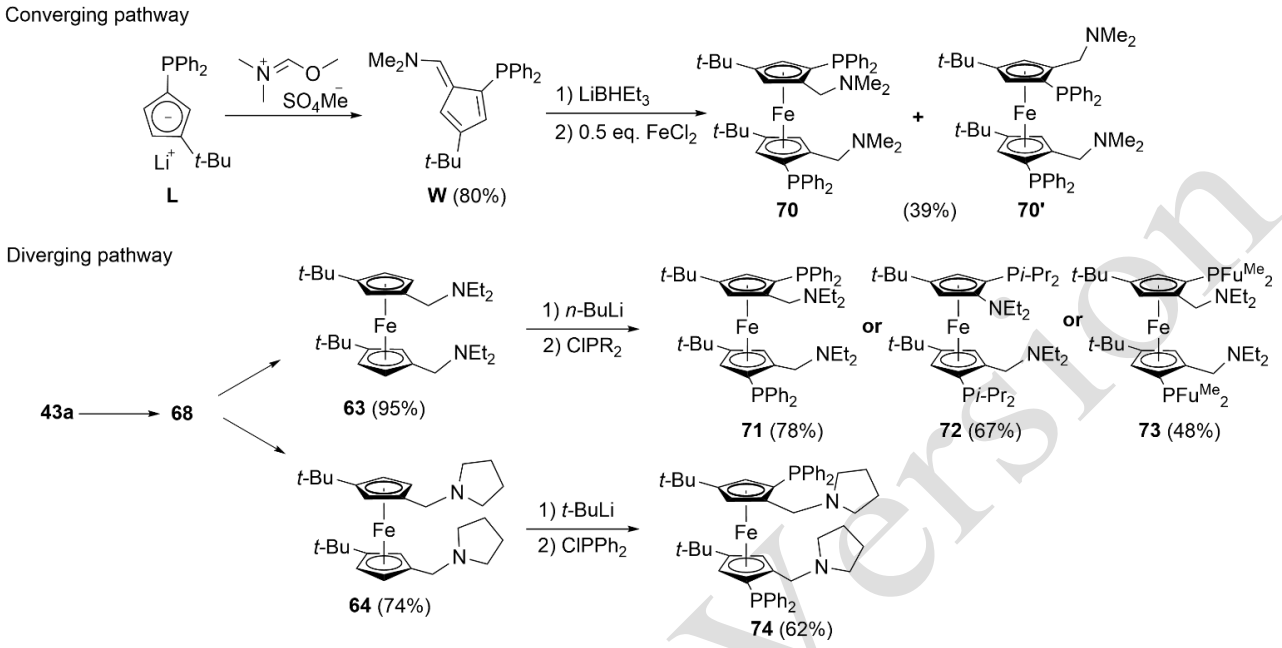

Figure 43. Converging and diverging routes towards hexafunctionalized ferrocene tetradentate (P,P,N,N)-ligands.

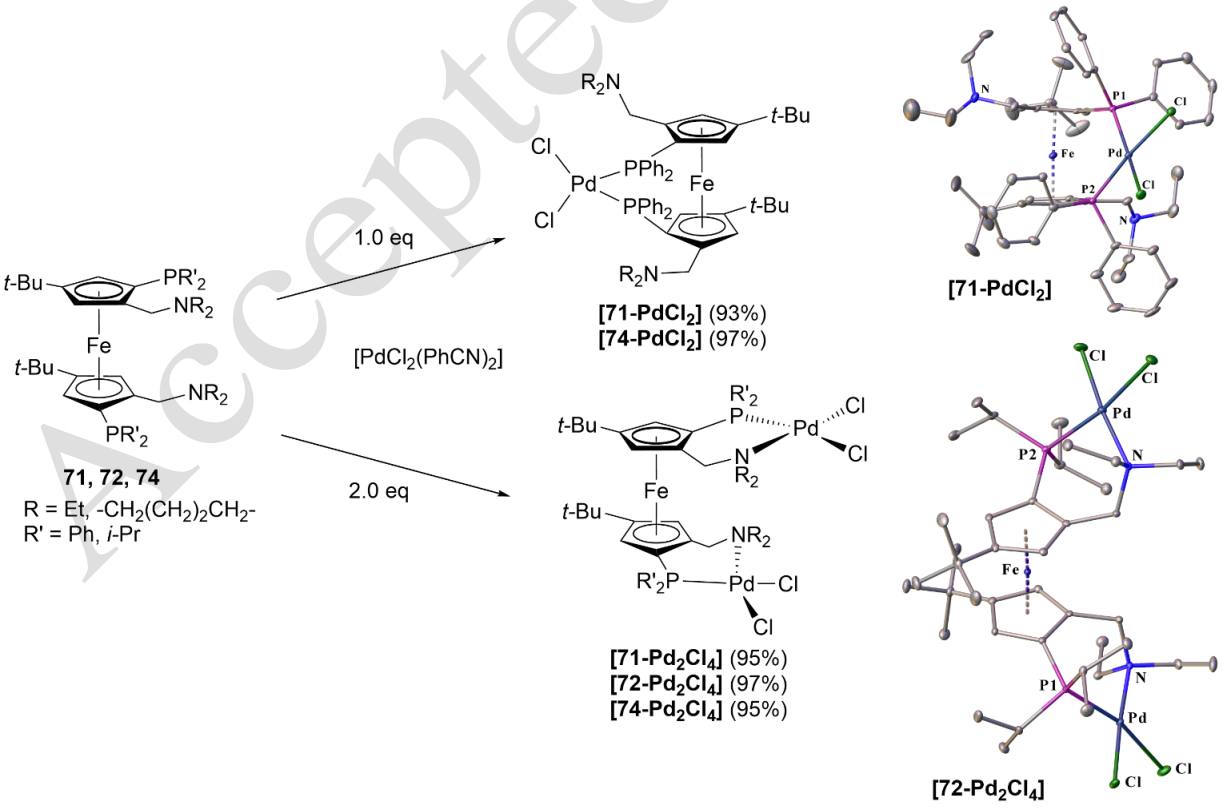

Figure 44. Mononuclear and dinuclear coordination modes of hexafunctionalized ferrocene tetradentate (P,P,N,N)-ligands to palladium.[62,68]

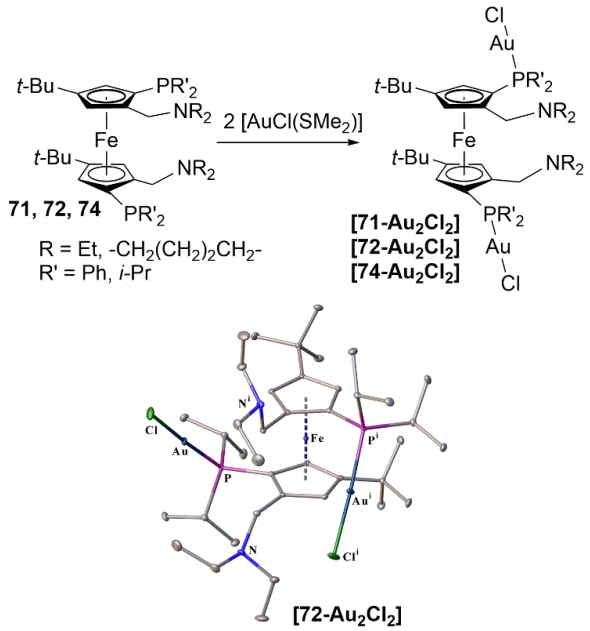

Figure 45. Dinuclear coordination mode of hexafunctionalized ferrocene tetradentate (P,P,N,N)-ligands to gold [symmetry transformation: (i) 1-x, +y, 1/2-z (**[72–Au_2Cl_2]**)].

The dinuclear gold(I) complexes obtained from tetradentate (*N*,*N*')-diamino-(*P*,*P*')-disphosphino ferrocene hybrid ligands **71**, **72** and **74** have been studied in the rare non-palladium Suzuki catalysis arylation of iodoarenes (Figure 46). Notably, gold(I) complexes have the same d^{10} electronic configuration as Pd(0), Ni(0) and Pt(0), which can be typical catalysts for C–C bond cross-coupling reactions. The ability of gold to undergo two-electron redox elementary steps such as oxidative addition (O.A.) was recently demonstrated in some challenging sp^2-C–I oxidative addition.[70] Accordingly, the complex **[72–Au_2Cl_2]** bearing electron-rich isopropyl groups on phosphorus was able to catalyze Suzuki coupling with a very good selectivity of heterocoupled product. Isolated molecularly-defined gold dinuclear complexes were used, but we also checked the absence of contaminant metal traces and especially palladium on the commercial K_2CO_3 used. No palladium was detected above the apparatus limit of 0.15 ppm. Therefore, **[72–Au_2Cl_2]** had a noticeable reactivity in the arylation of *ortho*-substituted iodoarenes bearing different substituents: electron-rich, electron poor and even towards hindered polyphenyl (Fig. 46). Based on the (P,N)-ferrocene ligands, this catalytic system tolerated various valuable functional groups on iodoarenes, and contributed toward demonstrating the potential of gold complexes in elementary steps of cross-coupling reactions traditionally attributed to d^{10} metal(0) complexes.

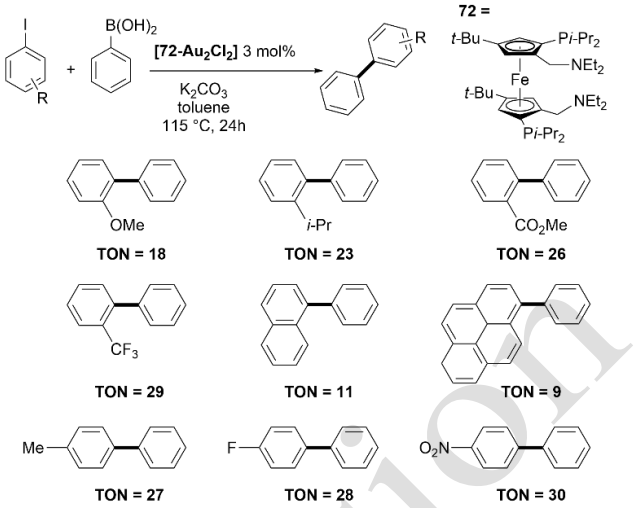

Figure 46. Gold-catalyzed Suzuki arylation of hindered iodoarenes.

4. Ambiphilic Ferrocenes

Molecules combining Lewis acids and Lewis bases on a same scaffold can lead to valuable cooperative reactivity. These ambiphilic molecules (also named frustrated Lewis pairs) have shown great interest in hydrogen splitting and metal-free hydrogenation reactions, or for the activation of *C1* small molecules (CO_2) as well as in coordination chemistry.[71,72] Phosphines or amines are commonly associated to boranes or alanes. Various organic scaffolds have been used, but only few metallocene-bridged ambiphiles have been developed. Owing to its stability and flexibility, we used ferrocene as a linker for synthesizing diborane, phosphino-borane and amino-borane derivatives. Our expertise in the field of constrained polyphosphine ferrocenes and the development of these new ambiphilic ferrocenes inspired us for synthesizing new class of hybrid ferrocenes bearing both a Lewis base (phosphine) and a Brønsted acid or polar function (carboxylic acid). Hybrid ferrocenes of this type are viewed as potential hemilabile ligands exploitable in coordination chemistry and metal catalysis.[2,73,74]

4.1. Ferrocenyl Boranes and (P, B)- and (N, B)-Hybrids

In studies conducted in cooperation with G. Bouhadir and D. Bourissou, bis-Lewis acidic diborylferrocenes were synthesized *via* the assembling at metal salt of preformed Cp rings.[60]

Borylcyclopentadienyl lithium salts **X–Y** were obtained from sequential lithiation/borylation of dimethylfulvene and then reacted with iron dichloride provides to form complexes **76–77** in 61–93% (Figure 47).[60] In contrast to the diverging synthesis of diphosphino ferrocenes described above (Figs. 23, 25 and 30), this synthesis was surprisingly fully diastereoselective and only led to the formation of the *rac* diastereoisomer.

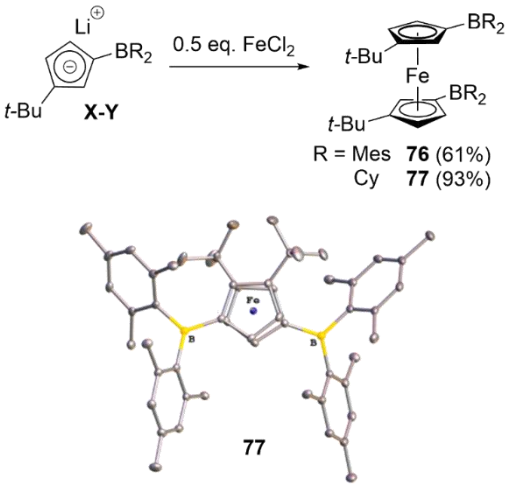

Figure 47. Diastereoselective synthesis of diborylferrocenes.

The origin of this unanticipated diastereoselectivity has been studied by DFT calculation. The potential energy surface was investigated so as to identify and compare the diastereoisomers and conformers. The origin of the stereoselectivity was attributed to steric repulsions which are minimized between the *tert*-butyl and the $BMes_2$ groups in the eclipsed conformation of the racemic form. The boryl Cps rings **X–Y** allow also the synthetic extension to other metallocenes as illustrated by the formation of cobaltocene **78** (Figure 48). DFT calculation showed, here also, that the energy formation of *meso* diastereoisomer is higher of *ca* 6 kcal mol^{-1} than the one found for the preferred eclipsed *rac* diastereoisomer.

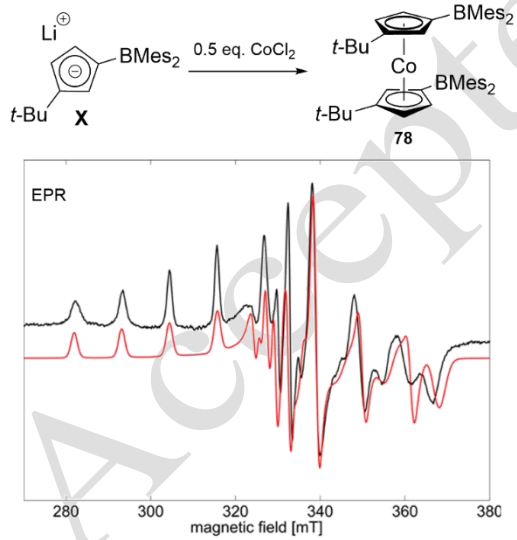

Figure 48. Synthesis of diborylcobaltocene **78** and EPR spectra (experimental in black, simulated in red).

The diastereoselectivity favoring the eclipsed *rac* diastereoisomer has been confirmed by the comparison of computed and simulated EPR spectra of the various isomers with the experimental EPR spectrum recorded. The electronic structure of cobaltocene **78** was analyzed by EPR. The spin density of this open-shell complex is mainly localized on the Co center, spin density is also found on the boron atoms indicating partial delocalization of the unpaired electron over the Lewis acid moieties. Consistently, the singly occupied molecular orbital is a combination of a Co-centered 3d orbital with π(BC) orbitals on each $CpBMes_2$ rings. There is no significant direct M···B interaction in **76–78**. [60]

To take advantage of the possible cooperativity between neighboring sites, we became interested in ambiphilic compounds featuring three or more functional groups directly bonded to the ferrocene platform. The boryl Cp **X** was used for the synthesis of such an ambiphile, this by a mixed Cp assembling inspired by the synthesis of mixed triphosphines (see section 2.2). The assembling at iron dichloride of bis(diphenyl)phosphino Cp **B** and *tert*-butylated boryl Cp **X** led to the formation of an unprecedented 1,2,1'-(P,P,B)-bis(diphenyl)phosphinoborylferrocene, **79**, in 32% yield (Figure 49).[75]

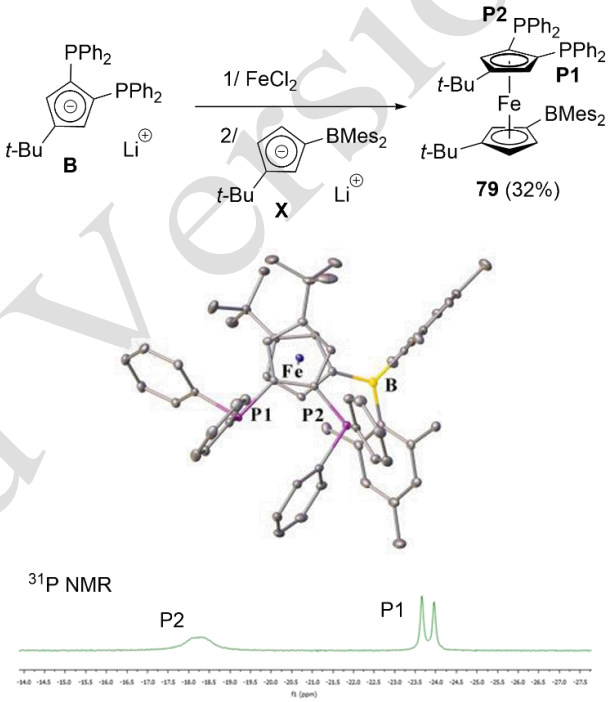

Figure 49. Synthesis and ^{31}P NMR (243 MHz, 300 K, $CDCl_3$) and XRD of 1,2,1'-(P,P,B)-bis(diphenylphosphino)borylferrocene **79**.

Tritopic ligand **79** bears five bulky groups on the ferrocene backbone. The spatial distribution of the substituents, analyzed in the solid state by XRD, is optimized with the two cyclopentadienyl rings nearly eclipsed with a cisoid arrangement of the *tert*-butyl groups. The three heteroatoms are oriented in the same direction in this conformation, opposite to the *tert*-butyl groups and the phosphorus atoms are in very different environments with P2 proximate to boron ($d_{P2\cdots B}$ = 4.239(2) Å). In comparison with related phosphino-boryl-ferrocenes with P···B distances ranging from 4.106(3) to 6.731(3) Å, see below, this distance is in the low range.[62,76–78]. The proximity of P2 and B, induces a steric congestion from which effects are also visible in ^{31}P NMR with an unusual very broad signal at –18.2 ppm, while a net doublet is observed for the other P1 atom (–23.8 ppm, $^3J_{PP}$ = 60 Hz). Hindered rotation around the Fc–B bond of **79** for P2 was shown to be responsible for this effect (inequivalent mesityl groups at B were evidenced by ^1H NMR). The strong 60 Hz magnitude of the J_{P1P2} coupling suggested some “through-space” (TS) spin coupling in line with the relatively short internuclear distance $d_{P1\cdots P2}$ = 3.871(2) Å. A

contribution of a *J* "through-space" component was further supported by the solvent-dependence of the $^{3}J_{P1P2}$ coupling noticed when replacing chloroform with toluene (from 60 to 44 Hz).

Coordination of the diphosphino boryl ferrocene **79** with platinum was easily achieved in quantitative yield (Figure 50). Despite its five sterically demanding substituents compound **79** preserves enough conformational flexibility to allow the chelating coordination of the two phosphorus atoms to platinum. The boron atom sensibly moved away from phosphorus P2 ($d_{P2\cdots B}$ = 5.294(7) Å), and accordingly the corresponding ^{31}P NMR signal get resolved in a well-defined singlet at 22.0 ppm (Fig. 50). No Lewis acid–metal Pt···B interaction was observed like in some other more constrained phosphinoborylferrocene platinum complexes.[79–81]

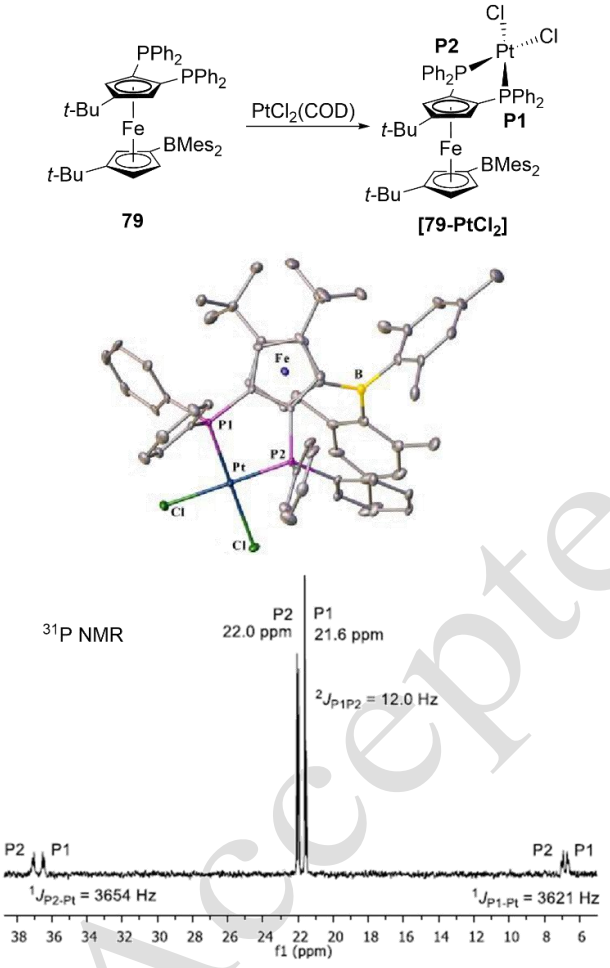

Figure 50. Coordination of the diphosphino boryl ferrocene **79** with platinum

Tetrafunctionalized dialkylated (P, B)- or (N, B)-ambiphiles were prepared by sequential lithiation/electrophilic trapping from 1,1'-dibromo-3,3'-di-*tert*-butyl-ferrocene **56** (Figure 51). We found this synthetic pathway to be more efficient and selective than assembling from *tert*-butylated boryl cyclopentadienides, which is still also feasible. Monolithiation/phosphination of **56** leads to the formation of **80–82** in 43–76% yield. The targeted dialkylated boryl phosphino ferrocenes **83–87** were then obtained in 35–99% yield by lithiation/borylation of **80–82** (Fig. 51). [62,63]

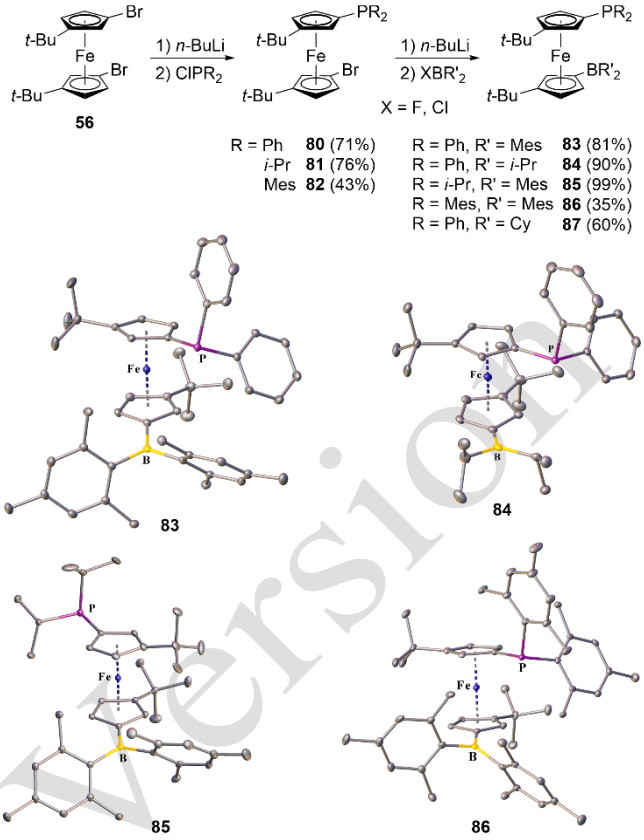

Figure 51. Synthesis of borylphosphinoferrocenes **83–87**.

The diastereoselective stepwise modification of di-*tert*-butylated ferrocenes took also profit for this class of compounds of the separation of electroactive species from **56** after controlled electrolysis (see section 2.4).[58] The bulky *tert*-butyl groups on ferrocene platform induced planar chirality of ambiphiles and enforced closer proximity of antagonist Lewis functions. The systematic structural analysis of compounds **83-86** in the solid state showed that ambiphiles **83**, **84** and **86** were in a cisoid conformation of the heteroatoms, while compound **85** adopted a transoid arrangement. The introduction of bulky *tert*-butyl groups in general favored a closer proximity between the phosphine/borane pairs, however, this was not systematically the case, as seen for instance with **85** ($d_{P2\cdots B}$ = 6.731(3) Å). Therefore, the ferrocenyl platform in any case clearly conserved a certain degree of rotational flexibility. Yet, for all these ambiphiles, X-ray and NMR did not evidence any P→B pair closing.

By using reductive amination on the precursor **88** which was obtained in two steps of lithiation/formylation from dibromoferrocene **56** (60% yield, Figure 52), the aminobromoferrocenes **89–90** were isolated in 76–86% yield. Then aminoborylferrocenes **91–92** were synthesized by sequential lithiation/borylation of **89–90** in 15–20% yield without further optimization of the reactions (Fig. 52).[62]

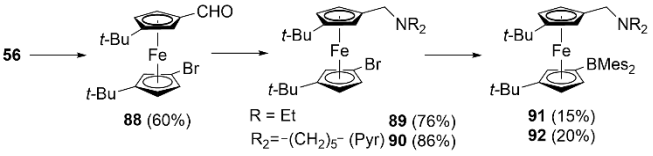

Figure 52. Synthesis of aminoborylferrocenes **91–92**.

Thus, we provided a robust method, fully diastereoselective, to produce highly functionalized sterically constrained 1,1'-planar chiral (P, B)-ferrocene ambiphiles. For these, in addition scale up in multigram amounts was reached by a purification mode taking advantage of ferrocene backbone redox properties through controlled electrolysis. The extension to a new class of (N,B)–ferrocene ambiphiles as well as (P,P)– and (P,N)–hybrids (potentially hemilabile compounds)[62] illustrates the general interest of this synthetic chemistry. This constrained class of ligands has a potential which remains to be explored/exploited as frustrated Lewis Pairs (FLPs), and in intramolecular cooperative chemical reactivity or coordination chemistry.

4.2. *tert*-Butylated phosphanyl carboxylic acids and derivatives

Building on the successful development of highly functionalized phosphino-boryl ferrocenes **83**-**87**, we further addressed the challenging preparation of ditopic polar hybrid ferrocene analogs such as *tert*-butylated phosphanyl carboxylic acids and their corresponding aldehydes. These hybrid ambiphilic species combines Brönsted-acidic and Lewis-basic functional moieties in their structure. Ferrocenophane opening method by PhLi was employed for the synthesis of *tert*-butylated ferrocene **94** bearing phosphine and carboxylic acid in 5% isolated yield (Figure 53).[82] This synthetic pathway is limited concerning the nature of phosphorus substituent beyond a phenyl group, and undergone significant purification troubles due to phosphine oxidation.

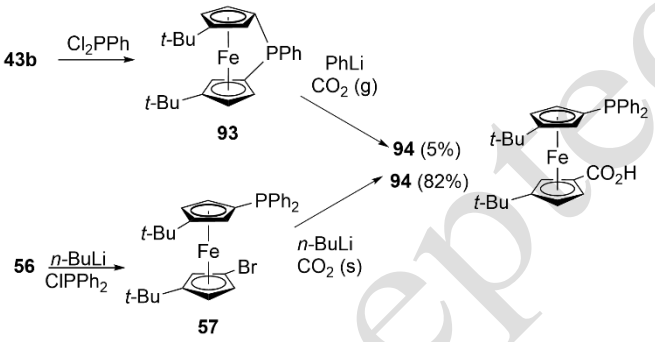

Figure 53. Synthetic pathways to phosphinoferrocene carboxylic acid **94**.

We thus applied the post-functionalization pathway from **56** to achieve phosphino-carboxylic acid **94** and **99-101**. The lithiation of bromophosphino ferrocene **57** followed by the reaction with solid CO_2 gave **94** in a much higher 82% yield (Fig. 53).[82] Electron-rich phosphines were protected from oxidation by adduct formation with BH_3, before the lithiation/carboxylation step. We thus synthesized dicyclohexyl and di(*iso*-propyl) analogous **100** and **101** by lithiation and carboxylation of the protected bromophosphino ferrocenes **97** and **98** (Figure 54). Essentially, the phosphine ferrocene bromide intermediates could be isolated in their free or in P-protected form as borane adducts, which are both suitable for further synthesis. This was illustrated by the preparation of the corresponding aldehydes **102-104**.

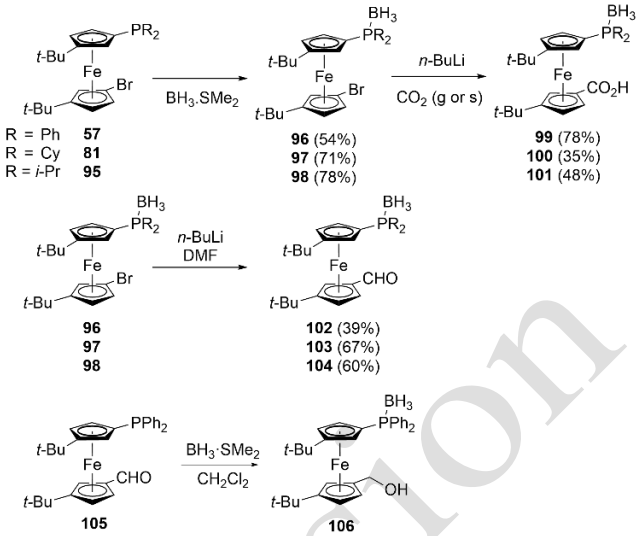

Figure 54. Synthesis of electron-rich phosphinoferrocene carboxylic acids **100–101** and analogous aldehydes **102–104**.

The aldehyde function of compound **105** can be reduced in alcohol and the phosphine protected by the one-pot use of $BH_3{\cdot}SMe_2$ in excess, providing alcohol **106**. In the case of acid **99**, we also achieved removal of borane protecting group to form **94** by using conventional methods with 1,4-diazabicyclo-[2.2.2]octane (DABCO, 2.2 equiv) in toluene (80°C, 18 h) or refluxing 10 h in ethanol.

In relation with the successful gold-catalyzed Suzuki reaction with dinuclear gold stabilized by hybrid 1,1'-(P,N)-ferrocene ligands (see section 3.2), the coordination of phosphino-carboxylic acid **94** with gold was investigated, and easily achieved in quantitative yield (Figure 55). The mononuclear gold complex presented a linear P–Au–Cl geometry [angles found to be 178.04(5) ° and 176.45(5) °] for the two similar molecules present in the unit cell. Interestingly, the changed conformation of the ferrocene ligand in the gold complex resulted in close proximity between the Brönsted acidic carboxylic function and the gold center. We observed proximity between gold and oxygen atoms with $d_{Au\cdots O=COH}$ of 3.509(4) and 3.442(3) Å, and distances Au···C(O)OH of 3.777(5), 3.720(4) Å). The proximity of oxygen atoms from the metallic center may have an influence in catalytic processes.

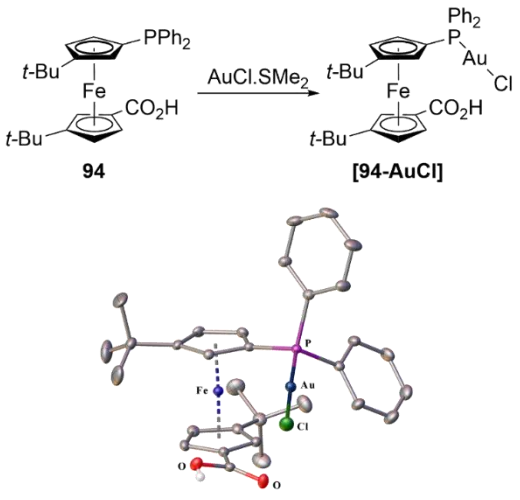

Figure 55. Coordination of **94** with gold.

In these highly functionalized hybrid compounds, besides intramolecular steric interactions, the polarity of carboxylic acids in both ligands and complexes induce significant intermolecular hydrogen bonding, which controls the supramolecular assembly of the ferrocene derivatives in the solid state. Further applications in gold and palladium catalysis are under investigation.

5. The icing on the cake: the ferrocene hexaphosphine and its coordination modes

Only few ferrocenyl phosphine ligands of higher rank than diphosphines are known. While ferrocene derivatives substituted with three or four groups incorporating donor atoms were early on developed in our group, we extended cyclopentadienyl functionalization to the introduction of three phosphino groups based on three successive sequences of phosphination/lithiation of cyclopentadienyl lithium.[83] The tris-(diphenylphosphino) cyclopentadienide lithium salt **Z** was obtained from **F** in 56% yield (Figure 56). The reaction of this highly substituted cyclopentadienyl with $FeCl_2$ led to the formation of the unique ferrocenyl hexaphosphine **107** in 65% yield. The ^{31}P CD_2Cl_2 solution NMR pattern of **107** at 25°C displayed two broad signals at –24.5 and –29.8 ppm. Down to –60°C, the fluxional behavior of the hexaphosphine is slowed down and well-defined signals in a 1:2 ratio appeared as a triplet at –26.0 ppm and a doublet at –31.2 ppm (J_{PP} = 37 Hz). The ^{31}P NMR pattern at low temperature is consistent with the XRD structure of the hexaphosphine of *C2h* molecular symmetry. The Cp rings of the ferrocene platform have a staggered position, leading to a piano-stool arrangement for the two sets of three phosphorus atoms. The coupling constant J_{PP} = 37 Hz between heteroannular phosphorus is a nonbonded coupling constant “through-space”, arising from the overlap of the electron clouds of the lone-pairs of phosphorus pointing towards each other and consistent with the X-ray structure. Accordingly, short spatial distances between P atoms are observed: $d_{P1\cdots P2}$ = 3.9121(6) Å, $d_{P1\cdots P3}$ = 3.9756(6) Å and $d_{P2\cdots P3}$ = 3.4083(5) Å.

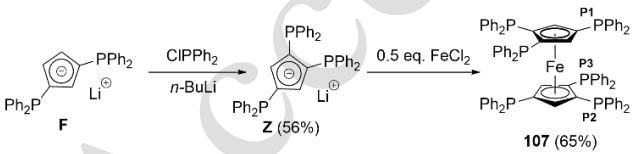

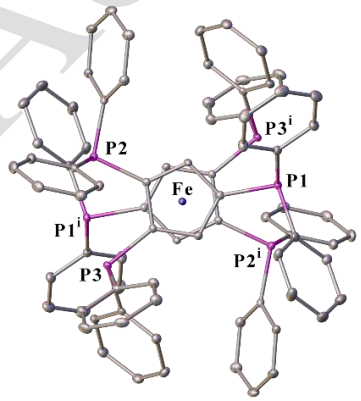

Figure 56. Synthesis and XRD structure of the hexaphosphine **107** [symmetry transformation: (i) 2-x -y 2-z].

The outstanding fluxionality of the hexaphosphine was exploited in coordination chemistry. The six phosphino groups allowed an unmatched versatility in coordination to transition metals. Coordination of **107** with molybdenum and rhodium lead to binuclear species, in which, each metal center is coordinated by three phosphines conserving the piano-stool conformation of the ligand (**107–$Mo_2(CO)_6$** and **107–$Rh_2Cl_2(CO)_2$**, Figure 57, top).

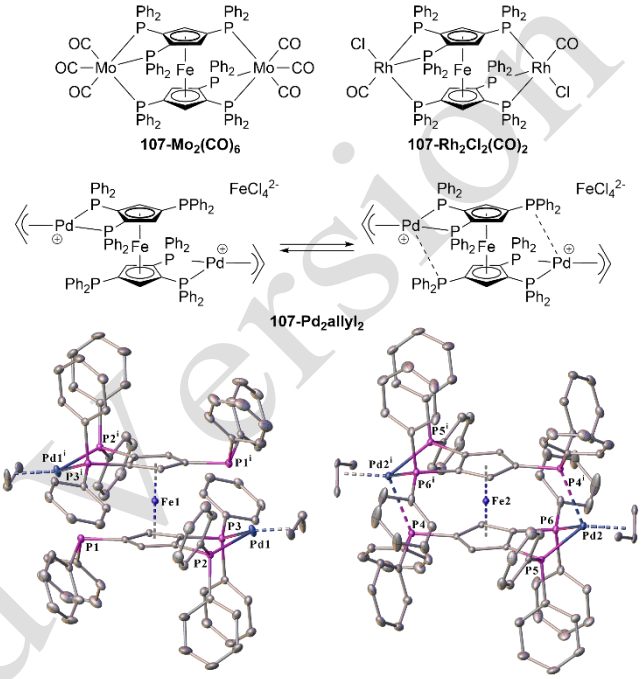

Figure 57. Dinuclear complexes of hexaphosphine **107** with transition metals [symmetry transformations: (i) 1-x, 1-y, 1-z (left) and -x, -y, -z (right)].

Unexpectedly, the reaction of hexaphosphine with a Pd(II) allylic complex, in the presence of $FeCl_2$, can lead to the formation of two cationic binuclear isomeric species (formula [{Pd(η^3-allyl)}$_2$**107**][$FeCl_4$]), named [**107–Pd_2allyl$_2$**], and identified by XRD for which two structures are present in the unit cell (Fig. 57, bottom). In the first isomer, while the bis-chelation of Pd(II) formed the expected square-planar structure “P_2Pd–L”, a labile P–Pd bond is observed with the heteroannular phosphorus. In the complexes the P–Pd distances are similar for the chelating pairs (ranging between 2.305 and 2.349 Å). Conversely, a short Pd–P distance is observed for the third phosphorus atom in the pentavalent Pd isomeric complex (2.618 Å) indicating the presence of a bonding interaction that does not exist in the other isomer (Pd⋯P distance of 2.988 Å). This was not due to any distortion of hexaphosphine within the conformers since essentially similar distances and angles are found, not to special packing. Thus, the structural features of the palladium complex indicate that in hexaphosphine **107** the ferrocene backbone allows enough flexibility for the third phosphorus atom to interact in a labile way with a strongly P-chelated Pd(II) centre in a square-planar environment. This experimentally observed bonding situation reminds some calculated stabilized resting state in Pd(0) after reductive elimination from C–O bond formation in catalytic etherification (section 2.2, **P** Fig.19). Despite the presence of this third P–Pd bond, the strongly P-

chelated Pd(II) center remained in a quasi-square-planar environment.

Hexaphosphine **107**, which mainly serves as a double triphosphine with molybdenum, rhodium and palladium, operates a remarkable coordination change with platinum(II), in which the use of this heavy metal clearly highlights the flexibility capacity of the ferrocene backbone (**107−Pt_2Cl_2**, Figure 58).

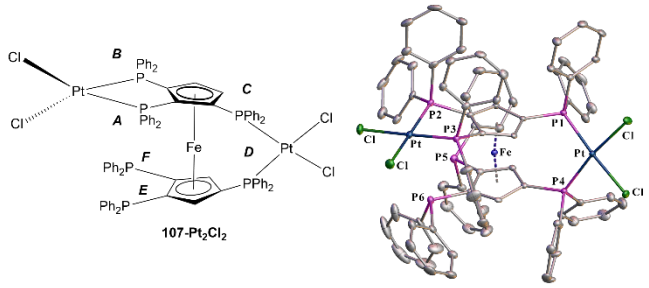

Figure 58. Dinuclear complexes of hexaphosphine **107** with transition metals.

In **107−Pt_2Cl_2** a Pt(II) dichloride moiety is coordinated in a 1,2-homoannular mode, while the second Pt(II) center is coordinated in a 1,1'-heteroannular mode by non-vicinal phosphines. This was made possible by a combination of rotation and tilting of the Cp rings. This happened despite the high steric hindrance due to the presence of six phosphino groups. The two platinum centers are in different square-planar environments. A representative difference is the wide angle found for the coordination of the heteroannular phosphorus pair at platinum, P1–Pt1–P4 = 98.99(4) °, compared to the narrower bite angle P2–Pt2–P3 = 85.23(4) ° for the coordination of the homoannular phosphorus pair. Though 1,2-homoannular and 1,1'-heteroannular coordination schemes are classical of metallocene-based ligands coordination, hexaphosphine **107** is a rare example of a metallocene derivative coordinating in both modes,[17] with additional two phosphino groups still available for further coordination. Hexaphosphine **107** is able to adopt a variety of coordination mode representative of its outstanding flexibility despite its high functionalization at Cp rings. Its capacity to provide heteropolymetallic original complexes remains to be exploited.

7. Conclusion and Outlook

Over the period 2003-2018 the chemistry of ferrocenyl polyphosphines allowed developing catalytic applications with palladium(0), in which the crucial role of polydentate interactions was elucidated by ^{31}P NMR and kinetic measurements. This reactivity was extended recently to gold(I) catalyzed cross-coupling. Perspectives in nickel chemistry are rather appealing. Intriguing fundamental knowledge in chemical physics related to nonbonded “through-space” nuclear spin-spin couplings was also gathered, and should be further addressed in the future by computational methods. The synthesis of many new cyclopentadienyl-based reagents (including Cp-boryl and amines), of original di-, tri-, tetra- and hexaphosphine, as well as their corresponding coordination complexes with group 6 to 11 transition metals has been described. Our library of phosphine ligands extended to unique tetradentate (P, N)-hybrids, as well as ambiphilic (P, B)- and (N, B)-ferrocenes in which dialkylated structures allows for some conformational control of the ferrocenyl platform. Diverging and converging routes allowed to identify some highly diastereoselective synthetic methods. The development of other hybrids like polar species holding carboxylate would be in the future extended to sulfonates and other functions that would help cooperative catalysis in aqueous or polar media. Future work will seek to produce other densely functionalized ferrocene-based compounds with the ultimate goal of triggering reactivity and new ligand behavior also owing to the redox properties of the ferrocene moiety.

CCDC 1961440 (for **[71-$PdCl_2$]**) and 1961441 (for **[71-Pd_2Cl_4]**) contain the supplementary crystallographic data for this paper. These data can be obtained free of charge from The Cambridge Crystallographic Data Centre.

Acknowledgments

This work was supported by the ANR-PRC 2016 program (ALCATRAS, ANR-16-CE07-0001-01), the CNRS, Université de Bourgogne, the Région Bourgogne Franche Comté (Excellence program CHIMENE and ISITE-BFC program COMICS) and the fonds européen de développement regional (FEDER). The IUF is sincerely thanked for supporting JCH. Our works benefited from the help of many talented partners from various topics in chemical sciences, including the groups of I. R. Butler (Wales), H. Doucet (Rennes), D. Lucas (Dijon), M. Saeys (Singapore), P. H Toy (Hong-Kong), D. Bourissou (Toulouse), and P. Štěpnička (Prague). Our works benefited from the help of many talented partners from various topics in chemical sciences, including the groups of I. R. Butler (Bangor), H. Doucet (Rennes), D. Lucas and C. Devillers (Dijon), M. Saeys (Singapore), P. H Toy (Hong-Kong), D. Bourissou (Toulouse) and P. Štěpnička (Prague). The students and coworkers who participated to these works are warmly thanked (especially: A. Fihri, M. Beaupérin, S. Mom, V. V. Ivanov and R. Smaliy).

Keywords: Ferrocenylphosphines · Functionalization ·Hybrid ligands · Coordination compounds · XRD Structure

[1] K. S. Gran, T. S. A. Hor, in *Ferrocenes Homog. Catal. Org. Synth. Mater. Sci.* (Eds.: A. Togni, T. Hayashi), VCH Verlagsgesellschaft, Weinheim, Germany, **1995**.
[2] P. Štěpnička, *Ferrocenes: Ligands, Materials and Biomolecules*, John Wiley & Sons, **2008**.
[3] I. R. Butler, *Eur. J. Inorg. Chem.* **2012**, *2012*, 4387–4406.
[4] L.-X. Dai, X.-L. Hou, Eds. , *Chiral Ferrocenes in Asymmetric Catalysis: Synthesis and Applications*, Wiley-VCH, Weinheim, **2010**.
[5] T. J. Colacot, *Chem. Rev.* **2003**, *103*, 3101–3118.
[6] T. Ireland, G. Grossheimann, C. Wieser-Jeunesse, P. Knochel, *Angew. Chem. Int. Ed.* **1999**, *38*, 3212–3215.
[7] We sincerely apologize for this selection of names. Please note also that numerous German and British groups and other developed ferrocene chemistry (Manners, Manoury, Erker, Siemling, Lang, Wagner, Togni, Long, Heinze, Hey-Hawkins and others).
[8] J. Boichard, J. Tirouflet, *Comptes Rendus Séances Académie Sci.* **1960**, 1394–1396.
[9] J. Tirouflet, G. Tainturier, R. Dabard, *Bull. Soc. Chim. Fr.* **1963**, 2403–2405.
[10] P. Dixneuf, R. Dabard, *Comptes Rendus Séances Académie Sci. Ser. C Sci. Chim.* **1968**, 1244–1246.
[11] D. Astruc, R. Dabard, *Comptes Rendus Séances Académie Sci. Ser. C Sci. Chim.* **1971**, 1248–1251.
[12] B. Gautheron, R. Broussier, *Bull. Soc. Chim. Fr.* **1971**, 3636–3642.

[13] R. C. J. Atkinson, V. C. Gibson, N. J. Long, *Chem. Soc. Rev.* **2004**, *33*, 313–328.
[14] J.-C. Hierso, R. Amardeil, E. Bentabet, R. Broussier, B. Gautheron, P. Meunier, P. Kalck, *Coord. Chem. Rev.* **2003**, *236*, 143–206.
[15] J.-C. Hierso, R. Smaliy, R. Amardeil, P. Meunier, *Chem. Soc. Rev.* **2007**, *36*, 1754–1769.
[16] I. R. Butler, L. J. Hobson, S. M. E. Macan, D. J. Williams, *Polyhedron* **1993**, *12*, 1901–1905.
[17] D. A. Thomas, V. V. Ivanov, I. R. Butler, P. N. Horton, P. Meunier, J. C. Hierso, *Inorg. Chem.* **2008**, *47*, 1607–1615.
[18] R. Broussier, S. Ninoreille, C. Legrand, B. Gautheron, *J. Organomet. Chem.* **1997**, *532*, 55–60.
[19] R. Broussier, S. Ninoreille, C. Bourdon, O. Blacque, C. Ninoreille, M. M. Kubicki, B. Gautheron, *J. Organomet. Chem.* **1998**, *561*, 85–96.
[20] R. Broussier, E. Bentabet, R. Amardeil, P. Richard, P. Meunier, P. Kalck, B. Gautheron, *J. Organomet. Chem.* **2001**, *637–639*, 126–133.
[21] J.-C. Hierso, A. Fihri, V. V. Ivanov, B. Hanquet, N. Pirio, B. Donnadieu, B. Rebière, R. Amardeil, P. Meunier, *J. Am. Chem. Soc.* **2004**, *126*, 11077–11087.
[22] J.-C. Hierso, D. Evrard, D. Lucas, P. Richard, H. Cattey, B. Hanquet, P. Meunier, *J. Organomet. Chem.* **2008**, *693*, 574–578.
[23] J.-C. Hierso, *Curr. Org. Chem.* **2011**, *15*, 3197–3213.
[24] J.-C. Hierso, D. Armspach, D. Matt, *C. R. Chim.* **2009**, *12*, 1002–1013.
[25] J.-C. Hierso, *Chem. Rev.* **2014**, *114*, 4838–4867.
[26] B. E. Cowie, F. A. Tsao, D. J. H. Emslie, *Angew. Chem. Int. Ed.* **2015**, *54*, 2165–2169.
[27] S. Sadeh, M. P. T. Cao, J. W. Quail, J. Zhu, J. Müller, *Chem. – Eur. J.* **2018**, *24*, 8298–8301.
[28] J.-C. Hierso, A. Fihri, R. Amardeil, P. Meunier, H. Doucet, M. Santelli, B. Donnadieu, *Organometallics* **2003**, *22*, 4490–4499.
[29] E. André-Bentabet, R. Broussier, R. Amardeil, J.-C. Hierso, P. Richard, D. Fasseur, B. Gautheron, P. Meunier, *J. Chem. Soc. Dalton Trans.* **2002**, 2322–2327.
[30] M. Beaupérin, E. Fayad, R. Amardeil, H. Cattey, P. Richard, S. Brandès, P. Meunier, J.-C. Hierso, *Organometallics* **2008**, *27*, 1506–1513.
[31] V. Rampazzi, J. Roger, R. Amardeil, M.-J. Penouilh, P. Richard, P. Fleurat-Lessard, J.-C. Hierso, *Inorg. Chem.* **2016**, *55*, 10907–10921.
[32] J.-C. Hierso, M. Beaupérin, P. Meunier, *Eur. J. Inorg. Chem.* **2007**, 3767–3780.
[33] D. Evrard, D. Lucas, Y. Mugnier, P. Meunier, J.-C. Hierso, *Organometallics* **2008**, *27*, 2643–2653.
[34] C. Amatore, M. Azzabi, A. Jutand, *J. Organomet. Chem.* **1989**, *363*, C41–C45.
[35] C. Amatore, M. Azzabi, A. Jutand, *J. Am. Chem. Soc.* **1991**, *113*, 8375–8384.
[36] V. A. Zinovyeva, S. Mom, S. Fournier, C. H. Devillers, H. Cattey, H. Doucet, J.-C. Hierso, D. Lucas, *Inorg. Chem.* **2013**, *52*, 11923–11933.
[37] V. A. Zinovyeva, C. Luo, S. Fournier, C. H. Devillers, H. Cattey, H. Doucet, J.-C. Hierso, D. Lucas, *Chem. Eur. J.* **2011**, *17*, 9901–9906.
[38] A. Jahel, N. V. Vologdin, N. Pirio, H. Cattey, P. Richard, P. Meunier, J.-C. Hierso, *Dalton Trans.* **2008**, 4206–4208.
[39] M. Beauperin, R. Smaliy, H. Cattey, P. Meunier, J. Ou, P. H. Toy, J.-C. Hierso, *Chem. Commun.* **2014**, *50*, 9505–9508.
[40] M. Beaupérin, R. Smaliy, H. Cattey, P. Meunier, J. Ou, P. H. Toy, J.-C. Hierso, *ChemPlusChem* **2015**, *80*, 119–129.
[41] M. Beaupérin, A. Job, H. Cattey, S. Royer, P. Meunier, J.-C. Hierso, *Organometallics* **2010**, *29*, 2815–2822.
[42] M. Platon, N. Wijaya, V. Rampazzi, L. Cui, Y. Rousselin, M. Saeys, J.-C. Hierso, *Chem. Eur. J.* **2014**, 20, 12584–12594.
[43] V. V. Ivanov, J. C. Hierso, R. Amardeil, P. Meunier, *Organometallics* **2006**, *25*, 989–995.
[44] R. V. Smaliy, M. Beaupérin, H. Cattey, J. Roger, H. Doucet, Y. Coppel, P. Meunier, J.-C. Hierso, *Organometallics* **2009**, *28*, 3152–3160.
[45] M. Platon, L. Cui, S. Mom, P. Richard, M. Saeys, J.-C. Hierso, *Adv. Synth. Catal.* **2011**, *353*, 3403–3414.
[46] S. Mom, M. Beaupérin, D. Roy, S. Royer, R. Amardeil, H. Cattey, H. Doucet, J. C. Hierso, *Inorg. Chem.* **2011**, *50*, 11592–11603.
[47] J.-C. Hierso, A. Fihri, R. Amardeil, P. Meunier, H. Doucet, M. Santelli, V. V. Ivanov, *Org. Lett.* **2004**, *6*, 3473–3476.
[48] J.-C. Hierso, V. V. Ivanov, R. Amardeil, P. Richard, P. Meunier, *Chem. Lett.* **2004**, *33*, 1296–1297.
[49] J.-C. Hierso, M. Beaupérin, P. Meunier, *Eur. J. Inorg. Chem.* **2007**, 3767–3780.
[50] H. Doucet, J.-C. Hierso, *Angew. Chem. Int. Ed.* **2007**, *46*, 834–871.
[51] J. Roger, S. Mom, M. Beaupérin, S. Royer, P. Meunier, V. V. Ivanov, H. Doucet, J.-C. Hierso, *ChemCatChem* **2010**, *2*, 296–305.
[52] M. Platon, J. Roger, S. Royer, J.-C. Hierso, *Catal. Sci. Technol.* **2014**, *4*, 2072–2080.
[53] S. Mom, M. Platon, H. Cattey, H. J. Spencer, P. J. Low, J.-C. Hierso, *Catal. Commun.* **2014**, *51*, 10–14.
[54] D. Roy, S. Mom, M. Beaupérin, H. Doucet, J.-C. Hierso, *Angew. Chem. Int. Ed.* **2010**, *49*, 6650–6654.
[55] D. Roy, S. Mom, D. Lucas, H. Cattey, J.-C. Hierso, H. Doucet, *Chem. – Eur. J.* **2011**, *17*, 6453–6461.
[56] G. Trouve, R. Broussier, B. Gautheron, M. M. Kubicki, *Acta Crystallogr. Sect. C* **1991**, *47*, 1966–1967.
[57] R. Broussier, E. Bentabet, P. Mellet, O. Blacque, P. Boyer, M. M. Kubicki, B. Gautheron, *J. Organomet. Chem.* **2000**, *598*, 365–373.
[58] S. Ninoreille, R. Broussier, R. Amardeil, M. M. Kubicki, B. Gautheron, *Bull. Soc. Chim. Fr.* **1995**, *132*, 128–138.
[59] J. Roger, S. Royer, H. Cattey, A. Savateev, R. V. Smaliy, A. N. Kostyuk, J.-C. Hierso, *Eur. J. Inorg. Chem.* **2017**, *2017*, 330–339.
[60] E. Lerayer, P. Renaut, S. Brandès, H. Cattey, P. Fleurat-Lessard, G. Bouhadir, D. Bourissou, J.-C. Hierso, *Inorg. Chem.* **2017**, *56*, 1966–1973.
[61] A. Fihri, J.-C. Hierso, A. Vion, D. H. Nguyen, M. Urrutigoïty, P. Kalck, R. Amardeil, P. Meunier, *Adv. Synth. Catal.* **2005**, *347*, 1198–1202.
[62] E. Lerayer, P. Renaut, J. Roger, N. Pirio, H. Cattey, C. H. Devillers, D. Lucas, J.-C. Hierso, *Chem. Commun.* **2017**, *53*, 6017–6020.
[63] E. Lerayer, P. Renaut, J. Roger, J.-C. Hierso, *Fr. Demande*, **2015**, FR 3014871 (A1).
[64] R. Broussier, S. Ninoreille, C. Bourdon, O. Blacque, C. Ninoreille, M. M. Kubicki, B. Gautheron, *J. Organomet. Chem.* **1998**, *561*, 85–96.
[65] R. Broussier, E. Bentabet, M. Laly, P. Richard, L. G. Kuz'mina, P. Serp, N. Wheatley, P. Kalck, B. Gautheron, *J. Organomet. Chem.* **2000**, *613*, 77–85.
[66] F. Allouch, N. Dwadnia, N. V. Vologdin, Y. V. Svyaschenko, H. Cattey, M.-J. Penouilh, J. Roger, D. Naoufal, R. Ben Salem, N. Pirio, J.-C. Hierso, *Organometallics* **2015**, *34*, 5015–5028.
[67] N. Dwadnia, J. Roger, N. Pirio, H. Cattey, J.-C. Hierso, *Coord. Chem. Rev.* **2018**, *355*, 74–100.
[68] http://www.theses.fr/2017UBFCK050; Thesis N. Dwadnia **2017**.
[69] N. Dwadnia, J. Roger, N. Pirio, H. Cattey, R. Ben Salem, J.-C. Hierso, *Chem. – Asian J.* **2017**, *12*, 459–464.
[70] M. Joost, A. Zeineddine, L. Estévez, S. Mallet−Ladeira, K. Miqueu, A. Amgoune, D. Bourissou, *J. Am. Chem. Soc.* **2014**, *136*, 14654–14657.
[71] D. W. Stephan, G. Erker, *Angew. Chem. Int. Ed.* **2015**, *54*, 6400–6441.
[72] G. Bouhadir, D. Bourissou, *Chem. Soc. Rev.* **2016**, *45*, 1065–1079.
[73] P. Štěpnička, *Chem. Soc. Rev.* **2012**, *41*, 4273–4305.
[74] N. Dwadnia, J. Roger, N. Pirio, H. Cattey, J.-C. Hierso, *Coord. Chem. Rev.* **2018**, *355*, 74–100.
[75] E. Lerayer, P. Renaut, J. Roger, N. Pirio, H. Cattey, P. Fleurat-Lessard, M. Boudjelel, S. Massou, G. Bouhadir, D. Bourissou, J.-C. Hierso, *Dalton Trans.* **2019**, *48*, 11191–11195.
[76] M. W. P. Bebbington, S. Bontemps, G. Bouhadir, M. J. Hanton, R. P. Tooze, H. van Rensburg, D. Bourissou, *New J. Chem.* **2010**, *34*, 1556–1559.
[77] M. Abubekerov, P. L. Diaconescu, *Inorg. Chem.* **2015**, *54*, 1778–1784.
[78] A. Tlili, A. Voituriez, A. Marinetti, P. Thuéry, T. Cantat, *Chem. Commun.* **2016**, *52*, 7553–7555.
[79] B. E. Cowie, D. J. H. Emslie, *Chem. – Eur. J.* **2014**, *20*, 16899–16912.
[80] B. E. Cowie, D. J. H. Emslie, *Organometallics* **2015**, *34*, 4093–4101.
[81] S. Bontemps, M. Sircoglou, G. Bouhadir, H. Puschmann, J. A. K. Howard, P. W. Dyer, K. Miqueu, D. Bourissou, *Chem. – Eur. J.* **2008**, *14*, 731–740.
[82] L. Radal, P. Vosáhlo, J. Roger, H. Cattey, R. Amardeil, I. Císařová, P. Štěpnička, N. Pirio, J.-C. Hierso, *Eur. J. Inorg. Chem.* **2019**, *2019*, 865–874.
[83] R. V. Smaliy, M. Beaupérin, A. Mielle, P. Richard, H. Cattey, A. N. Kostyuk, J.-C. Hierso, *Eur. J. Inorg. Chem.* **2012**, *2012*, 1347–1352.

MINIREVIEW

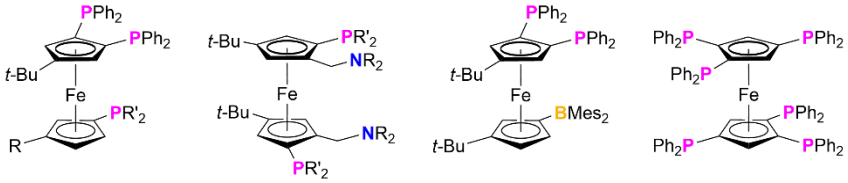

Ferrocene Chemistry

*E. Lerayer, L. Radal, T. A. Nguyen, N. Dwadnia, H. Cattey, R. Amardeil, N. Pirio, J. Roger, and J.-C. Hierso**

Highly Functionalized Ferrocenes

Highly functionalized ferrocenes, which include notably (P,P,P,P)-, (P,P,N,N)-, (P,P,P')-, (P,P,B)-, (P,B)- and (N,B)-compounds were developed in which the heteroatoms coexist in a close proximity on a common ferrocene platform with a controlled conformation.